Magnetohydrodynamics

PAUL H. ROBERTS
University of California, Los Angeles
Los Angeles, California, United States

PATRICK H. DIAMOND
University of California, San Diego
San Diego, California, United States

Glossary

Alfvén wave A wave that propagates along magnetic lines of force because of the tension of the field lines; also called a hydromagnetic wave.

Ampère's law The law that, in pre-Maxwell theory, determines the magnetic field created when electric current flows.

beta The name given to the ratio of the gas pressure to the magnetic pressure in a conducting fluid; plasma β is one of the figures of merit awarded to a magnetostatic equilibrium.

dynamo The process whereby a magnetofluid self-excites and amplifies a magnetic field.

electromotive force The electric field created by a changing magnetic field. Motive refers to its ability to move charge in a conductor (i.e., generate current).

Faraday's law The law that determines the electromotive force created by a changing magnetic field.

field line A curve that is everywhere parallel to the direction of the prevailing magnetic field; also called a line of (magnetic) force, it is part of a family of such lines, one of which passes through each point of space.

field line tension Part of the stress that a magnetic field **B** exerts on a medium and interpreted as a tension in a flux tube of B^2/μ_0, per unit cross-sectional area of the tube; μ_0 is the permeability of the medium.

figure of merit A number that quantifies the susceptibility of a plasma equilibrium to a certain type of magnetohydrodynamics instability.

flux tube See magnetic flux surface.

force-free field The field in a particular type of magnetostatic equilibrium in which the Lorentz force vanishes and in which field and current are parallel.

gradient A term used to indicate how rapidly a scalar or vector field changes with position. In the case of a scalar field, Φ, it is used to describe the vector field that is parallel to the direction in which Φ increases most rapidly; it is equal to the spatial rate of change of the scalar in that direction and is denoted by $\nabla\Phi$.

interchange-ballooning mode An instability driven by the combined effects of pressure gradient and average, or locally, unfavorable curvature of the field lines.

International Thermonuclear Experimental Reactor (ITER) a large-scale experiment, run by an international consortium, designed to study the physics of burning plasma.

kink safety factor A figure of merit quantifying the susceptibility of a plasma equilibrium to kink instability.

kink-tearing mode An instability driven by current gradients.

line of force A curve that is everywhere parallel to the direction of the prevailing magnetic field; also called a (magnetic) field line, it is part of a family of such lines, one of which passes through each point of space.

Lorentz force The force per unit volume on a fluid conductor that carries an electric current (density **J**) and lying in a magnetic field **B**; mathematically, it is the vector product of **J** and **B** and can also be represented by magnetic stresses.

magnetic helicity A property of a magnetic field that is preserved in the motion of a fluid that is a perfect electrical conductor.

magnetic pressure Part of the stress that a magnetic field **B** exerts on a medium and interpreted as an isotropic pressure $B^2/2\mu_0$, where μ_0 is the permeability of the medium.

magnetic reconnection The process by which a magnetofluid forms thin current layers that change the field line topology and dissipate magnetic energy.

magnetic relaxation The process by which a magnetofluid relaxes to its minimum energy state subject to certain constraints.

magnetic shear The rate at which the direction of a magnetic field changes with position **x**; a special case is used in plasma physics as a figure of merit.

magnetic stresses Stresses that are equivalent in their dynamical effect to the Lorentz force.

magnetic surface, also called a flux tube or a magnetic flux surface A surface composed of field lines so that the magnetic field, **B**, is everywhere tangential to it. The flux of **B** contained within the surface is the same everywhere along its length.

Ohm's law The law that states that the electric current density, **J**, produced in a motionless conducting medium by an electric field **E** is proportional to **E**. The constant of proportionality is the electrical conductivity of the medium.

pre-Maxwell theory The approximate form of electromagnetic theory that existed prior to Maxwell's discovery of displacement currents.

scalar product A convenient mathematical abbreviation used to describe a quantity derived from two vectors, **F** and **G**, and in magnitude is equal to the product of their magnitudes, |**F**| and |**G**|, and the cosine of the angle between them; it is written as $\mathbf{F} \cdot \mathbf{G}$.

Taylor relaxation The process proposed by J. B. Taylor whereby a magnetofluid relaxes to its minimum energy state subject to the constraint of constant global magnetic helicity.

toroidal Alfvén eigenmode (TAE) A particular type of Alfvén wave appropriate to toroidal geometry.

vector product A convenient mathematical abbreviation used to describe a vector that is perpendicular to two other vectors, **F** and **G**, and that in magnitude is equal to the product of their magnitudes, |**F**| and |**G**|, and the sine of the angle between them; it is written $\mathbf{F} \times \mathbf{G}$, where **F**, **G**, and $\mathbf{F} \times \mathbf{G}$ form a right-handed triad.

Magnetohydrodynamics (*MHD*) is the study of the movement of electrically conducting fluids in the presence of magnetic fields. The magnetic field influences the fluid motion through the Lorentz force, which is proportional and perpendicular to the magnetic field and the electric current flowing through the conductor: The magnetic field is affected by the electric current created by an electromotive force which is proportional and perpendicular to the magnetic field and the fluid velocity. It is this duality between magnetic field and fluid flow that defines the subject of MHD and explains much of its fascination (and complexity).

1. INTRODUCTION

Magnetohydrodynamics (MHD) is the marriage of hydrodynamics to electromagnetism. Its most famous offspring is the Alfvén wave, a phenomenon absent from the two subjects separately. In fact, many consider the discovery of this wave by Alfvén in 1942 to mark the birth of MHD. Initially, MHD was often known as hydromagnetics, but this term has largely fallen into disuse. Like MHD, it conveys the unfortunate impression that the working fluid is water. In reality, the electrical conductivity of water is so small that MHD effects are essentially absent. Moreover, many fluids used in MHD experiments are antipathetical to water. Even as fluid mechanics is now more widely employed than hydrodynamics the terms magnetofluid mechanics or magnetofluid dynamics, which are already sometimes employed, may ultimately displace MHD. Magnetofluid is already widely used in MHD contexts.

Since electric and magnetic fields are on an equal footing in electromagnetism (EM), it may seem strange that the acronym EMHD was not preferred over MHD. There are two reasons for this. First, to invoke EM theory in its full, unapproximated form would, in most contexts, add complexity without compensating enlightenment. It usually suffices to apply the form of EM theory that existed in the 19th century before Maxwell, by introducing displacement currents, cast the theory into its present-day form. In this pre-Maxwell theory of EM, there are no displacement currents and the electric and magnetic fields are not on an equal footing; the magnetic field is the master and the electric field the slave. Consequently, MHD is an appropriate acronym, but EMHD is not. Situations in which this is untrue and in which full EM theory is needed involve relativistically moving fluids and are too seldom encountered to be described here; in this article, the pre-Maxwell approximation is used throughout. The second reason why EMHD cannot be used is that the acronym is generally understood to mean electron MHD, which studies the MHD of the electron fluid in a two-fluid description of a plasma, the ions forming the other fluid. This topic is also outside the scope of this article.

A significant branch of MHD is the study of Magnetostatic equilibria (MSE). This subject is the MHD analogue of hydrostatics, the branch of fluid mechanics that deals with fluids at rest, with the pressure gradient in the fluid balancing external forces such as gravity. Similarly, in MSE the fluid is motionless and the pressure gradient balances the Lorentz force (and any other forces present).

The two main applications of MHD are technological—to liquid metals and to plasmas. There is little doubt that the former has had the greater

impact on society. It includes the casting and stirring of liquid metals, levitation melting, vacuum-arc remelting, induction furnaces, electromagnetic valves, and aluminum reduction cells. Another application, the flow of a liquid metal in the blanket surrounding a thermonuclear reaction chamber, touches on the other main area: plasma MHD. The reactor contains a rarefied plasma of deuterium/tritium (DT) that is raised to a high enough temperature for these nuclei to fuse and release energy. The economic promise of such a device in generating magnetic fusion energy (MFE) has provided a powerful incentive for studying plasma MHD and has led to significant new insights, particularly into the structure and stability of MSE. In addition to these practical applications, the elucidation of a wide variety of magnetic phenomena in nature depends on an understanding of MHD. Astrophysics and geophysics provide abundant examples, including the magnetism of the earth, planets, and satellites, that of the sun and other stars, and that of galaxies.

This article describes the simplest form of MHD theory, in which the working fluid is a homogeneous, continuous medium. This may or may not (depending on context) be a satisfactory description of a plasma. In general, a plasma and its dynamics are described by kinetic equations that govern distribution functions for electrons, ions, and (if the plasma is incompletely ionized) neutral atoms. The distribution function, $f(\mathbf{x}, \mathbf{v}, t)$, of any of these species is proportional to the probablility that a particle of that species at position $\mathbf{x}$ is moving with velocity $\mathbf{v}$ at time t. In certain cases, such a description can be greatly simplified by replacing the kinetic equations for the functions f by a closed set of fluid equations. This happens when the dependence of each f on $\mathbf{v}$ is close to what it would be if the plasma were in local thermodynamic equilbrium, as seen by an observer moving with the mean velocity, $\mathbf{V}(\mathbf{x}, t)$, of the species at $\mathbf{x}$ and t. Such a distribution is termed Maxwellian. The distribution functions are then replaced by ion, electron, and neutral densities, n_i, n_e, and n_n, respectively, that give the total numbers of each species per unit volume at $\mathbf{x}$ and t, with each fluid having its own (mean) velocity. Although this may seem (and is) very complicated, it is far less forbidding than the alternative (i.e., solving for the evolution of the distribution functions).

The method of closure described previously necessarily involves an approximation of restricted validity. Single-fluid MHD also assumes that the characteristic length scale, $\mathscr{L}$, is large compared with the Debye length, $\mathscr{L}_{\text{debye}}$. This length quantifies the distance over which n_e and n_i can differ substantially from one another. When $\mathscr{L} \gg \mathscr{L}_{\text{debye}}$, these densities are closely equal and the plasma is very nearly electrically neutral. A second requirement for simple one-fluid MHD to hold is that $\mathscr{L}$ be large compared with the mean free path between particle collisions in the plasma and in comparison with the gyroradii. (A charged particle in a magnetic field would, in the absence of collisions with other particles, orbit about a field line in a spiral having a certain gyroradius that depends on its mass and charge and on the field strength.) These demands are more easily satisfied in many astrophysical contexts than in a thermonuclear reactor chamber. Nevertheless, one-fluid MHD can provide useful qualitative insights into the structure and stability of plasmas relevant to MFE.

To simplify the following discussion, the abbreviations shown in Table I will usually be employed. In particular, velocity means fluid velocity, density stands for the mass density of the fluid, field means magnetic field, current is short for electric current density, conductor means conductor of electricity, and potential means electric potential. Script letters—$\mathscr{L}$, $\mathscr{T}$, $\mathscr{V}$, $\mathscr{B}$, $\mathscr{J}$, $\mathscr{E}$, etc.—are used to indicate typical magnitudes of length, time, velocity, field, current, electric field, etc.

The aim of this article is to provide as simple an account of MHD as possible—one that is slanted toward the MFE field but one that involves a minimum of mathematics. Some familiarity with vector fields is necessary, however.

TABLE I
Abbreviations

Quantity	Symbol	Magnitude	SI unit
Time	t	$\mathscr{T}$	Seconds (s)
Position	$\mathbf{x}$	$\mathscr{L}$	Meters (m)
Velocity	$\mathbf{V}$	$\mathscr{V}$	m/s
Density	ρ	—	Kilogram/m^3 (kg/m^3)
Pressure	p	—	Newton/m^2 (N/m^2)
Temperature	T	—	Kelvin (K)
Field	$\mathbf{B}$	$\mathscr{B}$	Tesla (T)
Current	$\mathbf{J}$	$\mathscr{J}$	Amp/m^2 (A/m^2)
Charge density	v	—	Coulomb/m^3 (C/m^3)
Potential	Φ	—	Volt (V)
Electric field	$\mathbf{E}$	$\mathscr{E}$	V/m
Conductivity	σ	—	Siemens/m (S/m)

2. PRE-MAXWELL APPROXIMATION

Some readers may value a brief review of the relevant concepts in EM theory that underpin MHD; others may prefer to skim this section and move ahead to Section 3.

Under discussion are systems having characteristic length, time, and velocity scales, $\mathscr{L}$, $\mathscr{T}$, and $\mathscr{V}$, respectively, for which $\mathscr{L} \ll c\mathscr{T}$ and $\mathscr{V} \ll c$, where c is the speed of light. In these circumstances, EM phenomena are well described by an approximation that was in use before Maxwell introduced displacement currents and his famous equations into EM theory. This approximation, which is also called the nonrelativistic approximation (since it implies that c is infinite), is summarized.

Electrostatics is the study of static electricity. Each positive (negative) electric charge experiences an attraction toward every negative (positive) charge and a repulsion from every other positive (negative) charge. The sum, $\mathbf{f}$, of all these forces on a charge e is proportional to e and is conveniently represented by an electric field, $\mathbf{E} = \mathbf{f}/e$. Suppose that, in steady conditions, a test charge is carried around a closed curve Γ, where by test charge is meant a charge so small that it does not have any effect on the other charges. As the charge describes Γ, the agency that moves it will sometimes do work against the force $\mathbf{f} = e\mathbf{E}$ and will sometimes receive energy from it but, when the circuit is complete the net gain or loss of energy is zero. Such forces are termed conservative and this fact is expressed mathematically by the statement that $\mathbf{E} = -\nabla\Phi$, where Φ is the electric potential. (Here, $\nabla\Phi$ denotes the gradient of Φ, a vector that has Cartesian components $\partial\Phi/\partial x$, $\partial\Phi/\partial y$, $\partial\Phi/\partial z$.) If positive, $\Phi_1 - \Phi_2$ is the energy received from the electric field when a unit positive charge moves from a location where the potential is Φ_1 to one where the potential is Φ_2; if negative, it is the work that must be done to move the charge from the first location to the second. The force $\mathbf{f} = -e\nabla\Phi$ acts to move a positive charge in the direction of $\mathbf{E}$ from a region of higher potential to one of lower potential.

If a conductor carries a net charge, the mutual repulsion between charges quickly drives them to the surface of the conductor, where they arrange themselves with a surface charge density such that the surface is at a uniform potential Φ. The electric field is then normal to the surface and cannot move charges along the surface. The charge distribution is therefore static. Beneath the surface charge layer, $\mathbf{E}$ is identically zero, as is the volumetric charge density ϑ. If different areas of the surface are held at different potentials, as at the two ends of a straight wire, $\mathbf{E}$ is no longer zero in the conductor and a charge e experiences the force $\mathbf{f} = e\mathbf{E}$. If $e > 0$ (< 0) this moves it from (to) the area at the higher potential to (from) the area at the lower potential. The resulting flow of charge is called an electric current. Its density, $\mathbf{J}$, is proportional to the force $\mathbf{f}$ and, according to Ohm's law, it is given by $\mathbf{J} = \sigma\mathbf{E}$, where σ is the electrical conductivity of the conductor in siemens/meter (S/m). To relate this to the more familiar form of Ohm's law, consider again the example of the straight wire. If its length is L meters, a potential difference of Φ volts between its ends creates an electric field of strength Φ/L (V/m) and therefore a current of density $J = \sigma\Phi/L$ A/m^2. If the cross-sectional area of the wire is A, the total current is $I = JA = \sigma A\Phi/L = \Phi/R$, where $R = L/\sigma A$ is the electrical resistance of the wire in ohms (Ω). This result, $I = \Phi/R$, is the form of Ohm's law encountered in elementary texts on electricity and magnetism.

In pre-Maxwell theory, the flow of charge resembles the flow of a constant density fluid, for which mass conservation requires that the net flow of mass into any closed volume is equal to the net flow out of that volume. In the same way, charge conservation requires that the inward flow of electric current into the volume balances its outward flow.

Whenever current flows, a magnetic field, $\mathbf{B}$, attends it. This is shown in Fig. 1, again for a straight wire C having a circular cross section of radius a. In this case, $\mathbf{B}$ is in the θ direction, where θ is the azimuthal angle around the wire. Some lines of (magnetic) force are shown. A line of force, also called a field line, is actually not a line but a continuous curve whose tangent is everywhere

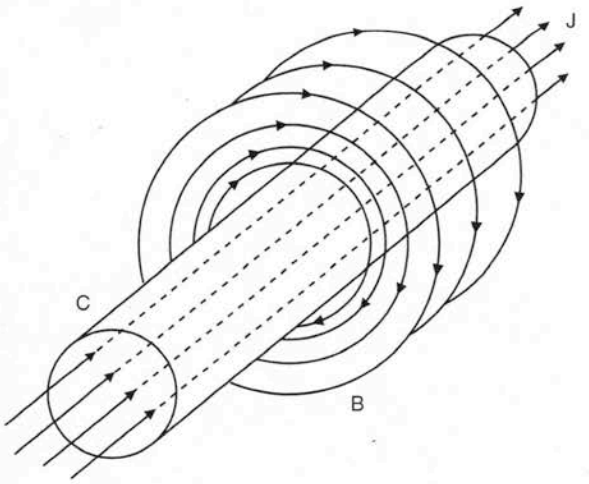

FIGURE 1 Lines of force created by a current-carrying wire C.

parallel to **B**. Although lines of force pass through every point in space, sketches such as Fig. 1 can only show a finite number. The density of lines indicates the strength of the field. Where lines bunch together (spread apart) the field is stronger (weaker). Magnetic charges, analogous to electric charges, do not exist. This means that a line of force may close on itself or cover a magnetic surface ergodically (i.e., without closing; Fig. 2), or it may continue to infinity, but it cannot terminate. It also means that (as for **J**) the net flow of **B** into any closed volume is equal to the net flow of **B** emerging from the volume. A bundle of lines of force contained in a magnetic surface form a flux tube (Fig. 3). The net flow of **B** into one end of a volume of the tube bounded by two of its cross sections is the same as the net flow that emerges from the other end. This is called the strength of the tube.

To determine **B** from **J** in a situation such as that sketched in Fig. 1, Ampère's law is required. This states that the component of **B** along any closed curve Γ is, when integrated around that curve, proportional to the net flux, I, of current through Γ. In a uniform medium, the constant of proportionality is its permeability, which in this article is always assumed to be the permeability of free space, $\mu_0 = 4\pi \times 10^{-7}$ H/m. (The fact that this value is exact is a quirk of the SI system of units, which makes use of one more quantity than is strictly necessary.) Taking the closed curve to be the (circular) line of force of radius r surrounding the wire, the required integral is $2\pi r B_\theta$, which by Ampère's law is also $\mu_0 I$, so that $B_\theta = \mu_0 I/2\pi r$; the field decreases with distance r from the wire as $1/r$. The field outside the wire does not depend on whether the current is uniform across the cross section of the wire ($J = I/\pi a^2$) or whether, as in a case considered in Section 3, it flows only along the surface of the wire with density $I/2\pi a$.

Faraday's law provides the final link between **B** and the electric field. This law applies to any closed curve Γ that is the periphery of a surface S. It states that the component of **E** along Γ, when integrated around Γ, is equal to the rate of decrease of the flux of **B** through S. This statement depends on a sign convention that can be understood from Fig. 4. If **E** is integrated around Γ in the direction of the arrows, then the flux of **B** through S is taken into the plane of the paper. (This right-handed rule also applies to Ampère's law; see Fig. 1.) Faraday's law shows that in unsteady EM states, **E** is not conservative (i.e., it cannot be expressed as $-\nabla\Phi$).

Faraday's law applies even when Γ is moving and changing shape, but in such cases **E** must be reinterpreted. To see why this is necessary, consider again Fig. 4. Suppose that **E** is zero and that **B** is uniform, constant in time and directed out of the plane of the paper. Now suppose that the sides *ad* and *bc* start to lengthen at speed U so that the area

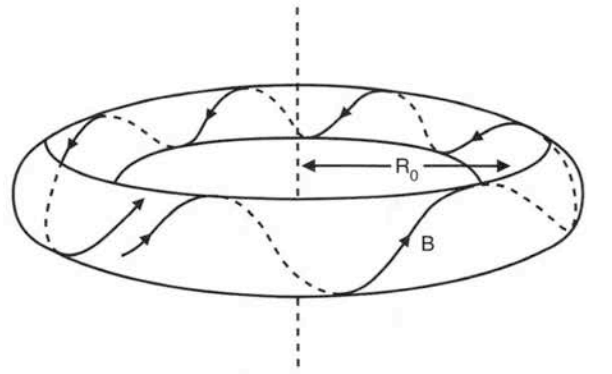

FIGURE 2 An axisymmetric magnetic surface filled ergodically by one line of force that does not close. The dashed line is the symmetry axis of the "donut"; it is also called the magnetic axis.

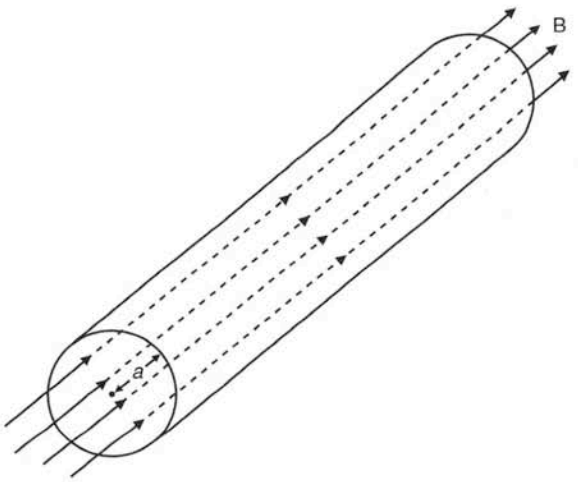

FIGURE 3 A straight flux tube. Its surface is composed of field lines.

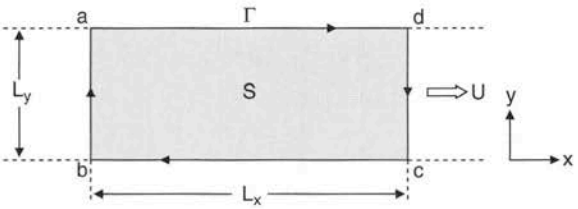

FIGURE 4 Application of Faraday's law to a growing rectangle S with periphery Γ. The sides *da*, *ab*, and *bc* are fixed. The side *cd* moves with speed U in the x direction. The sides *ad* and *bc* lengthen at the same rate.

S of the rectangle increases at the rate UL_y. The flux of B out of the plane of the paper increases at the rate BUL_y; in the positive sense defined previously, it decreases at the rate BUL_y. By Faraday's law, this must also be the integral of the component of the electric field along the sides of the integral. However, E is clearly zero on all sides of Γ, particularly on the stationary sides da, ab, and bc. One must conclude that when integrating the electric field around Γ, one is not integrating E_y on the moving side cd but some other electric field, E_y'. The required integral is then $E_y'L_y$ and Faraday's law gives $E_y' = -UB$.

This argument has uncovered a very significant fact: Although B (and J) are the same in all reference frames, the electric field is not. In the current example, $E_y' = -UB$ in the reference frame moving with speed U in the x direction. It is convenient here to make use of a shorthand notation: $\mathbf{U} \times \mathbf{B}$ is called the vector product of U and B. It is proportional and perpendicular to U and B; its Cartesian components are $U_yB_z - U_zB_y$, $U_zB_x - U_xB_z$, and $U_xB_y - U_yB_x$. In this notation, the electric field in the frame moving with the side cd is $\mathbf{E}' = \mathbf{U} \times \mathbf{B}$. More generally, when the electric field in one reference frame $\mathcal{F}$ is E, then it is $\mathbf{E}' = \mathbf{E} + \mathbf{U} \times \mathbf{B}$ in the reference frame $\mathcal{F}'$ moving with velocity U relative to $\mathcal{F}$. Returning to Faraday's law in the case in which Γ moves or changes shape, it is E′ and not E that is integrated around Γ, where E′ is evaluated at each point P of Γ using the velocity U at P.

The force on a charge e that is stationary in $\mathcal{F}'$ is $\mathbf{f} = e\mathbf{E}'$, which in $\mathcal{F}$ is more conveniently written as $\mathbf{f} = e(\mathbf{E} + \mathbf{U} \times \mathbf{B})$. Analogously, Ohm's law in a solid conductor moving with velocity U is $\mathbf{J} = \sigma(\mathbf{E} + \mathbf{U} \times \mathbf{B})$. To illustrate this modification of Ohm's law, suppose that the rectangle sketched in Fig. 4 is electrically conducting, with ad and bc being parallel rails along which cd slides, the electrical contact between cd and the rails being perfect. In general, a current I will flow around Γ in the direction indicated by the arrows. This current is driven through $cb + ba + ad$ by a potential difference Φ created by charges that accumulate at the sliding contacts c and d. At one extreme, when the resistance R_1 of $cb + ba + ad$ is large, $I = \Phi/R_1$ is small. By charge conservation, I is also the current flowing in cd and it is small because the electric field $E_y = (\Phi_c - \Phi_d)/L_y$ in cd created by the charges at c and d cancels out almost completely the electric field $-UB$ induced by the motion of cd; i.e., $|E_y'|$ is small. At the other extreme, when R_1 is small, the path $cd \rightarrow ba \rightarrow ad$ is almost a short-circuit, the contact charges at c and d are small, and these points are at nearly the same potential; E_y is small, $E_y' \approx -UB$, and the current $I = UBL_y/R_2$ flows around Γ in the direction indicated, where R_2 is the resistance of cd. In the general case between these two extremes, $I = UBL_y/R$, where $R = R_1 + R_2$ is the total resistance of Γ.

The modified Ohm's law also applies when the conductor is a fluid, but now U is replaced by the fluid velocity V, which is usually not the same everywhere. At a point at which the fluid velocity is V, the current density is $\mathbf{J} = \sigma(\mathbf{E} + \mathbf{V} \times \mathbf{B})$. By Ampère's law, this current will influence B. This fact exposes one half of the relationship between V and B, alluded to in Section 1, that characterizes the subject of MHD: Flow alters field in a fluid conductor. The other half of the relationship is a consequence of a force that a conductor experiences when J and B are nonzero. The force is proportional to, and perpendicular to, both J and B. This is the Lorentz force, $\mathbf{J} \times \mathbf{B}$ per unit volume. Through this force, field alters the flow of a fluid conductor.

To illustrate the action of the Lorentz force, consider the conducting rectangle Γ sketched in Fig. 4. The sides ab and cd experience equal and opposite forces in the x direction, IBL_y and $-IBL_y$ respectively. These oppose the continual expansion of the rectangle (an example of Lenz's law). To maintain the expansion, forces must be applied to the sides ab and cd, and these do work at the rate $UIBL_y = (UBL_y)^2/R = I^2R$, which is precisely the rate at which electrical energy is converted into heat in the circuit Γ by its electrical resistance R. In this way, mechanical energy is converted into electrical energy and then "ohmically" into heat.

To state this result more generally, it is convenient to introduce a second shorthand notation: $\mathbf{F} \cdot \mathbf{G}$ is the scalar product of two vectors F and G. In terms of their Cartesian components, it is $F_xG_x + F_yG_y + F_zG_z$. If $-\mathbf{V} \cdot (\mathbf{J} \times \mathbf{B})$ is positive at a point P, it quantifies the rate at which fluid loses its kinetic energy at P. This energy goes partially to increasing the magnetic energy density at P but some is radiated away from P through a "Poynting" energy flux $\mathbf{E} \times \mathbf{B}/\mu_0$. The remainder offsets the ohmic losses, J^2/σ per unit volume, at P. When $-\mathbf{V} \cdot (\mathbf{J} \times \mathbf{B}) > 0$ at P, the loss of kinetic energy provides a brake on the motion, which would cease even in the absence of viscous friction, unless maintained by some other force. When $-\mathbf{V} \cdot (\mathbf{J} \times \mathbf{B}) < 0$ at P, the reverse process occurs; field passes energy to motion, as in an electric motor.

The volumetric charge density ϑ in a moving fluid conductor is generally nonzero so that the fluid experiences a body force $\vartheta\mathbf{E}$ per unit volume. In the pre-Maxwell approximation, this is negligible in comparison with $\mathbf{J} \times \mathbf{B}$. These forces can be

reinterpreted in terms of stresses on the fluid and, not surprisingly, the electric stresses are negligible in comparison with the magnetic stresses. It is also found that the energy density of the electric field is insignificant compared with the energy density, $B^2/2\mu_0$, of the magnetic field. This highlights the unimportance of **E** relative to **B** in pre-Maxwell theory.

The magnetic stresses alluded to previously have two parts. One is an isotropic magnetic pressure, $p_M = B^2/2\mu_0$; the other is nonisotropic and can be interpreted as a field line tension of B^2/μ_0 per unit area, or AB^2/μ_0 for a flux tube of cross-sectional area A. Both parts increase quadratically with B. The magnetic pressure, which is already approximately 4 atm for a field of 1 T, is 10,000 times greater for $B = 100$ T.

The action of the field on the flow is recognized by including the Lorentz force $\mathbf{J} \times \mathbf{B}$ in the equation of motion that governs the fluid velocity **V**. The remaining forces affecting the motion include the gradient of the (kinetic) pressure p and a term, proportional to the (kinematic) viscosity ν, that describes frictional effects. When the Lorentz force is equivalently represented by magnetic stresses, the magnetic pressure p_M joins p in a "total" pressure $P = p + p_M$. The ratio $\beta = p/p_M = 2\mu_0 p/B^2$ is usually called beta. It is a significant quantity in plasma physics, where it is a figure of merit—one of several used to quantify the excellence or otherwise of a plasma containment device.

3. *IDEAL MAGNETOHYDRODYNAMICS AND MAGNETOSTATICS*

A fluid is termed ideal if it has zero viscosity and zero thermal conductivity but infinite electrical conductivity. Since **J** must be finite even though $\sigma = \infty$, Ohm's law $\mathbf{J} = \sigma(\mathbf{E} + \mathbf{V} \times \mathbf{B})$ implies that $\mathbf{E} = -\mathbf{V} \times \mathbf{B}$. Consequently, Alfvén's theorem holds: Lines of force move with the fluid as though frozen to it.

To establish this important result, let Γ be the periphery of a surface element S that moves with the fluid. Since $\mathbf{E}'$ vanishes everywhere on Γ, Faraday's law shows that the flux of **B** through S is unchanging. Suppose S is part of the curved surface C of a flux tube (Fig. 5A). The flux of **B** through S is zero because **B** is tangential to it; by Faraday's law, it remains zero as the contents of the flux tube are carried to a new location by the fluid motion **V**. Since this applies to every such S drawn on C, **B** remains tangential to C everywhere. Thus, it is still a flux tube at its new location. On shrinking the cross section of the tube to a single line of force, it is seen that this line of force moves with the fluid, as though frozen to it. A stronger statement can be made. Let Γ encircle the tube so that S becomes a cross section of the tube (Fig. 5B). The flux of **B** through S is the strength of the tube, as defined in Section 2. By Faraday's law, it is the same at its new location. This applies to every cross section. The fluid motion therefore preserves the strength of flux tubes and the integrity of the magnetic surfaces that contain them.

Alfvén's theorem provides a useful way of envisioning MHD processes in highly conducting fluids. For example, consider the eruption of a flux tube from the relatively dense region below the solar photosphere and into the more tenuous solar atmosphere (Fig. 6). Gravity drains the material in the ejected flux loop back to the solar surface, leaving the flux loop at low density and pressure, where it is in approximate equilibrium with its new surroundings. Such processes are responsible for expelling from the sun the field created within it.

Next, consider the way in which fluid motions can exchange energy with the field. Imagine a straight flux tube, initially of cross-sectional area A_0, lying in

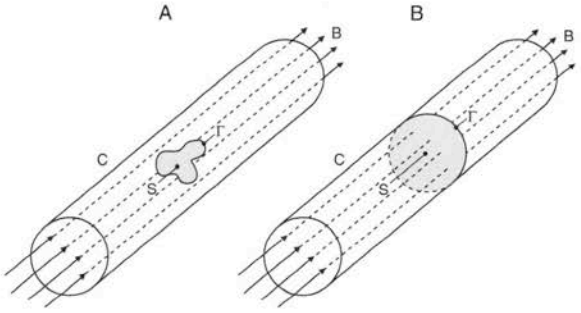

FIGURE 5 (A) An element S of surface area lying on the surface of a flux tube with periphery Γ. (B) A cross-section S of the flux tube with periphery Γ.

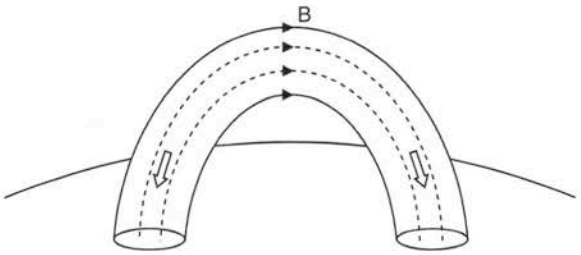

FIGURE 6 Fluid pulled by gravity down a flux tube that has erupted from the surface of the sun. Field directions are indicated by single arrows and fluid motion by arrowheads.

a compressible fluid. Suppose a motion compresses the tube uniformly so that, while remaining straight, its cross-sectional area is reduced to $A(<A_0)$. The density of the fluid it contains increases from its initial value of ρ_0 to $\rho = \rho_0(A_0/A)$. Since (by assumption) the fluid does not conduct heat, the tube compresses adiabatically, and its internal energy (i.e., the energy of the random molecular motions within it) increases so that its temperature rises. Because the strength of the tube cannot change, the field B_0 initially within the tube increases to $B = B_0A_0/A$ (i.e., by the same factor as ρ_0); thus, B/ρ remains at its initial value, B_0/ρ_0. The magnetic energy per unit length contained by the tube, however, increases from $A_0(B_0^2/2\mu_0)$ to $A(B^2/2\mu_0) = [A_0(B_0^2/2\mu_0)](A_0/A)$. In short, the kinetic energy of the compressing motion has been transformed into internal energy and magnetic energy. The reverse happens if $A > A_0$; the flux trapped in an intense tube tends to expand into surroundings where the field is weaker. For these reasons, sound traveling across a field moves faster (and much faster when β is small) than it would in the absence of the field; the magnetic pressure created by the field intensifies the restoring force in the compressions and rarefactions of the wave.

The transformation of kinetic energy into magnetic energy also occurs in an incompressible fluid when motions stretch field lines against their tension. The process may be likened to the storing of elastic energy in a stretched rubber band or to the energy transmitted to a violin string by plucking it. If the flux tube of cross-sectional area A_0 containing field B_0 considered previously is lengthened from L_0 to L, its cross section will decrease by the same factor ($A = A_0L_0/L$) and the field within it will increase by the same amount ($B = B_0L/L_0$). The magnetic energy it contains, which is proportional to B^2, is enhanced by a factor of $(L/L_0)^2$ from $(B_0^2/2\mu_0)L_0A_0$ to $(B^2/2\mu_0)LA = (B^2/2\mu_0)L_0A_0 = [(B_0^2/2\mu_0)L_0A_0](L/L_0)^2$. If $L = L_0 + \delta$, where $\delta \ll L_0$, the increase in magnetic energy is $(B_0^2/\mu_0)A_0\delta$. This is the work that the applied force had to do against the magnetic tension $(B_0^2/\mu_0)A_0$ of the field lines in stretching the tube by δ.

Tension has other important effects. Consider again the system shown in Fig. 1, but suppose now that the cylinder C is a compressible fluid or plasma surrounded by a vacuum. Suppose that the current I flows along the surface of C so that $I/2\pi a$ is the surface current density. The current I produces a field of strength $B_\theta = \mu_0 I/2\pi a$ on C. Because of their curvature, the field lines exert a "hoop stress" on C of $B_\theta^2/2\mu_0$ per unit area and directed radially inward. This compresses the fluid in C. Since $\mathbf{B}$ is zero in C, only (kinetic) pressure p can oppose the hoop stress. If $p = B_\theta^2/2\mu_0$, the forces are in balance, and the configuration is in *MSE*.

One may imagine that this MSE is brought about in the following way. Initially, A is large and p is small. After the current I and its associated field B have been set up, the forces on C are not in balance and the hoop stresses exerted by the field lines encircling C pinch the plasma column in much the same way as a stretched elastic band squeezes what it encircles. As these lines of force shorten and A becomes smaller, magnetic energy is converted into internal energy. The interior of C becomes hotter and its pressure p increases to oppose the further contraction of the field lines. Plausibly, the final result is an MSE of the kind envisaged previously, in which a plasma column has been strongly heated and prevented from expanding by the encircling field. Hot plasma is then confined within a magnetic bottle and away from solid walls. The possibility of this kind of magnetic confinement is of considerable interest in the MFE field. A hot reacting plasma must be prevented from leaching impurities from the solid walls of the reactor because these would greatly enhance the radiative losses, cooling the plasma and quenching the reactions.

In an MSE, the Lorentz force $\mathbf{J} \times \mathbf{B}$ balances the pressure gradient ∇p. This means that $\mathbf{B}$, being perpendicular to ∇p, is tangential to the constant–p surfaces, which are therefore magnetic surfaces, as defined in Section 2, and can be labeled by their value of p. Current lines (curves drawn parallel to $\mathbf{J}$) also lie on these surfaces and, like the field lines, they may close or traverse the surfaces ergodically. The total pressure P is continuous across the special magnetic surface that is the boundary of a plasma; if the exterior is a vacuum, P must balance the magnetic pressure, $B^2/2\mu_0$, in the vacuum.

If a region exists in which $\mathbf{J} \times \mathbf{B} = 0$, the field within it is termed force-free. Since $\nabla p = 0$, the pressure p is constant in the region, and p is no longer available to label surfaces on which the field and current lines are constrained to lie. Since $\mathbf{J}$ and $\mathbf{B}$ are parallel in a force-free field, $\mathbf{J} = \lambda\mathbf{B}$, where λ is constant on each field line, this being the component $J_\parallel = \mathbf{J} \cdot \mathbf{B}/B$ of $\mathbf{J}$ parallel to $\mathbf{B}$ on that line. The parameter λ may act as a surrogate for p in labeling the magnetic surfaces and constraining the field and current lines. If, however, λ is also constant, the field and current lines become unconstrained. A single field line and a single current line may fill the region. These are termed stochastic lines. They magnetically connect every part of the region to

every other part. Particular cases of this are presented in Sections 4.6 and 5.3.2.

The MSE just described is called the Z pinch because the current flows parallel to the axis of C, a direction usually labeled by z. The Z pinch is shown in Fig. 7A, together with two other MSEs. In Fig. 7B, the θ pinch, the current flows around the plasma column, a direction often denoted by θ. Between these extremes is the screw pinch (Fig. 7C). Here, the current flows in helices around C. The pitch $q_J = J_z/J_\theta$ of the helices depends on r, the radius of the cylindrical magnetic surface on which they lie. The field lines are also helices with a different pitch, q. The way that q varies with r is a significant factor for the stability of the equilibrium, and dq/dr is another figure of merit, called magnetic shear (see Section 5.3). It quantifies how rapidly the direction of the magnetic field changes as a function of r.

As applied to plasma devices, an obvious shortcoming of the linear or one-dimensional pinches shown in Fig. 7 is that, in practice, they must have ends, and these are sources of contamination. Greater interest therefore centers on toroidal or two-dimensional pinches. One may visualize a toroidal MSE as a linear pinch whose ends are joined together by bending it around on itself to form a donut of radius R_0, similar to that sketched in Fig. 2; R_0 is called the major radius and a the minor radius of the torus. The axis of symmetry is called the magnetic axis and distance from it is denoted by R. The z coordinate of the linear pinch is replaced by the angle ϕ around the magnetic axis, and increasing ϕ is called the toroidal direction. The coordinates r and θ of the linear pinch are approximately the same for both the linear and toroidal systems, r now being the distance from the axis running through the center of the donut and θ being the angle around that axis. Increasing θ is now called the poloidal direction. There is no toroidal MSE analogous to the θ pinch; in the absence of current flow in the toroidal direction, the Lorentz force cannot be balanced by a pressure gradient. Main interest centers on the toroidal screw pinch. The quantity $q = rB_\phi/R_0B_\theta$ is another figure of merit called the kink safety factor (see Section 5.3.2).

In addition to the one- and two-dimensional MSEs, there are also interesting three-dimensional configurations, so-called because they have no symmetry. Of fundamental concern in all these MSEs is the stability of the equilibria. This topic is discussed in Section 5.

Alfvén's theorem leads to a new phenomenon, the Alfvén wave. Consider again the straight flux tube of cross-sectional area A. Suppose first that the fluid is incompressible, and imagine that a transverse displacement bends the tube, carrying its contents with it, in obedience to the theorem (Fig. 8). The tension $\tau = AB^2/\mu_0$ of the tube acts, as in a stretched string, to shorten the tube. A wave results that moves in each direction along the tube with speed $V_A = \sqrt{(\tau/\Sigma)}$, where $\Sigma = \rho A$ is the mass per unit length of the string, with ρ being the fluid density. The wave velocity is therefore $\mathbf{V}_A = \mathbf{B}/(\mu_0\rho)^{1/2}$, which is usually called the Alfvén velocity. It is also the velocity with which energy can be transmitted along the field lines. In a compressible fluid, the situation is more complex because the presence of the field and its associated Lorentz force make sound propagation anisotropic. For example, the speed s of sound waves traveling parallel or antiparallel to the field $\mathbf{B}$ is unaffected by it: $s = \sqrt{\gamma p/\rho}$, where γ is the ratio of specific heats. For sound traveling perpendicular to the field, $s = \sqrt{(\gamma p + B^2/\mu_0)/\rho}$. For small β this is approximately V_A.

The MHD or Alfvénic timescale, $\tau_A = \mathscr{L}/V_A$, is very significant in many MHD contexts. It provides an estimate of how quickly a system responds to changes in its state. Such changes generate acoustic and Alfvén waves, the former crossing the system in a time of order $\tau_s = \mathscr{L}/s$, which for $\beta \ll 1$ is indistinguishable from τ_A. Thus, τ_A is the time required for the initial change to permeate the system. In particular, it is the dynamic timescale on which an MSE responds to a perturbation, and it is usually the timescale on which that equilibrium will, if unstable, be disrupted. It should be noted, however, that even if an equilibrium is stable according to ideal MHD, it

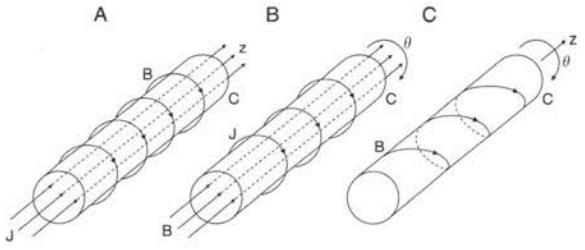

FIGURE 7 (A) Z pinch; (B) θ pinch; (C) screw pinch.

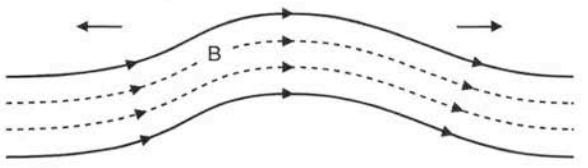

FIGURE 8 Alfvén wave propagation down a straight flux tube. The arrows indicate the directions of wave propagation.

may be unstable through diffusive effects ignored in ideal MHD. Such resistive instabilities are discussed in Section 5.

4. NONIDEAL MAGNETOHYDRODYNAMICS

4.1 Quantifying Deviations from the Frozen in Law

Alfvén's theorem poses a paradox: If field and fluid are inseparable, how did the fluid acquire its field in the first place? The answer is by diffusion, by which is meant, by diffusion of magnetic field. This happens because every real fluid has a finite conductivity.

In the reference frame $\mathscr{F}'$ moving with a particular point P of the fluid, Ohm's law is $\mathscr{J} = \sigma\mathscr{E}'$, in order of magnitude. Ampère's law shows that $\mathscr{J} = \mathscr{B}/\mu_0\mathscr{L}$, whereas Faraday's law implies that $\mathscr{E}' = \mathscr{B}\mathscr{L}/\mathscr{T}$. The timescale $\mathscr{T}$ on which **B** at P can change as P moves around is therefore the magnetic diffusion time, defined as $\tau_\eta = \mu_0\sigma\mathscr{L}^2 = \mathscr{L}^2/\eta$, where $\eta = 1/\mu_0\sigma$ is the magnetic diffusivity. On timescales $\mathscr{T}$ short compared with τ_η, the field is frozen to the fluid; for $\mathscr{T} \gg \tau_\eta$ it is not. Unless a field of scale $\mathscr{L}$ at P is maintained in some way, its lifetime is τ_η; also, a field of this scale cannot be implanted at P in a lesser time. One may consider these phenomenon as a type of EM memory that sets a minimum timescale for change, in the frame moving with the conductor.

Consider again the Z pinch described previously. After the potential difference has been applied between the ends of C at time $t = 0$, the current it creates initially flows only over the surface of C because, over short times, the plasma behaves as an ideal conductor in which **B** in the bulk of C cannot change from its initial zero value. Thereafter, the current sheet penetrates into C by diffusion, its thickness being of order $\delta_\eta = \sqrt{(\eta t)}$ at time t. After a magnetic diffusion time of $\tau_\eta = a^2/\eta$, the current will be distributed almost uniformly across the cross section of the column. As a digression, in practice the process may take rather longer since the diffusion of field into C is hampered by the increasing conductivity of the plasma as its temperature T rises through its adiabatic compression or heating. Similarly, the z–directed field initially trapped in a screw pinch grows as the column C collapses, whereas B_z in the surrounding vacuum does not. The tendency for the flux in C to diffuse out of the column is hampered by the diminishment of η that accompanies the compressional increase in T.

As another example, suppose that a plasma column C, such as the screw pinch shown in Fig. 7C, is contained within, but is not in contact with, a surrounding metallic wall. The field created outside C after the pinch has been initiated at time $t = 0$ cannot at first penetrate the walls because, over short times, they behave as perfect conductors in which **B** cannot change. The field is excluded from the walls by currents that flow in a thin skin on their surfaces, and these create their own field, which (when the walls are planar) is the mirror image of that of the plasma column (Fig. 9). The plasma column is repelled by its image (another example of Lenz's law), thus, preventing it from striking the wall. This stabilizing effect weakens in time because the thickness $\delta_\eta = \sqrt{(\eta t)}$ of the skin increases with t until ultimately the field completely penetrates the walls.

In a moving fluid, the advective timescale, $\tau_v = \mathscr{L}/\mathscr{V}$, quantifies the time taken (according to Alfvén's theorem) for a field of scale $\mathscr{L}$ to be carried over that distance. However, electrical resistance diffuses the field on a timescale of τ_η. If the magnetic Reynolds number, $Rm = \tau_\eta/\tau_v = \mathscr{L}\mathscr{V}/\eta$, is large, advection is more rapid than diffusion and Alfvén's theorem is useful in visualizing MHD processes. When $Rm \ll 1$, as is usually the case in technological applications of MHD involving liquid metals, the concept of frozen fields is not very useful. The prevailing field then provides an anisotropic friction that attempts to damp out motions perpendicular to itself on a timescale of $\tau_d = \rho/\sigma V_A^2 = \eta/V_A^2$, often called the magnetic damping time or the Joule damping time.

Energy can also be transmitted in a fluid by waves, and particularly significant for MHD systems is

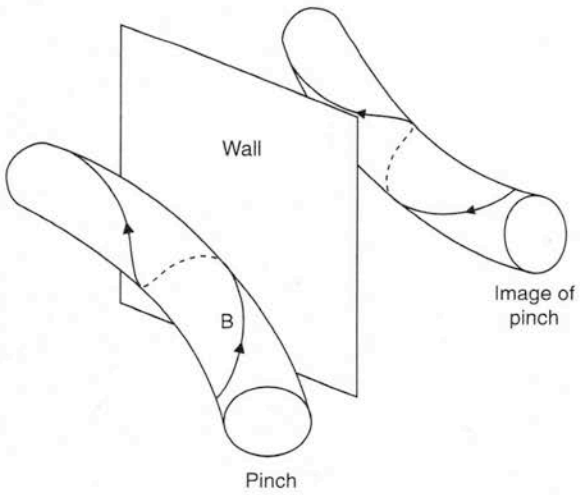

FIGURE 9 Image of a screw pinch in a conducting wall.

Alfvén radiation. This introduces a second way of quantifying diffusive effects: the Lundquist number, Lu. Alfvén waves are damped both by electrical conduction and by the viscosity ν of the fluid. The timescale over which this occurs is a combination $\tau_c = \mathscr{L}^2/(\eta + \nu)$ of τ_η and the viscous diffusion time, $\tau_\nu = \mathscr{L}^2/\nu$. For a liquid metal ($\nu \ll \eta$), $\tau_c \approx \tau_\eta$, and we shall now use τ_η in place of τ_c. During a time τ_η, the Alfvén waves travel a distance, $V_A\tau_\eta$. If the Lundquist number, $Lu = V_A\tau_\eta/\mathscr{L} = V_A\mathscr{L}/\eta$, is large, this distance greatly exceeds the characteristic length scale $\mathscr{L}$, and Alfvén radiation is significant. If $Lu \ll 1$, this is not the case since the time $\tau_d (= \eta/V_A^2)$ taken for the wave to damp out is small compared with the time $\tau_A (= \mathscr{L}/V_A)$ that the Alfvén wave requires to traverse the distance $\mathscr{L}$. The Lundquist number can be thought of as a magnetic Reynolds number, with the wave speed V_A replacing the advection speed $\mathscr{V}$.

4.2 Magnetic Reconnection

According to Alfvén's theorem, the topology of field lines cannot change in ideal MHD, but in a finitely conducting fluid ($\eta > 0$), field lines can sever and reconnect. This can happen fastest where scales are smallest (i.e., where the gradients of **B** are greatest). Magnetic reconnection is the process that forms thin current layers that change field topology and dissipate magnetic energy, even though the resistivity is modest and smoothly varying. Indeed, it is very important to distinguish magnetic reconnection, a process in which very thin (nearly singular) current sheets form in otherwise smoothly varying systems, from simple diffusive dissipation of magnetic energy when sharp profiles are built in *ab initio*. In magnetic reconnection, resistive diffusion and the magneto-fluid dynamics combine to release energy stored in the magnetic fields and to reconfigure the magnetic topology of the system. Reconnection phenomena are usually subdivided into two classes, namely driven magnetic reconnection (discussed here) and spontaneous magnetic reconnection (described in Section 5 in the context of the tearing instability).

Perhaps the simplest and most fundamental model of magnetic reconnection is that of Sweet and Parker, hereafter referred to as the Sweet–Parker reconnection (SPR) model. This is a two-dimensional machine that steadily reconnects field lines. A cross section is sketched at successive times in Fig. 10. Resistivity acts everywhere but is most effective near a segment of the x axis. To simplify the argument, it is supposed that $\eta = 0$ everywhere except in reconnection region (shown

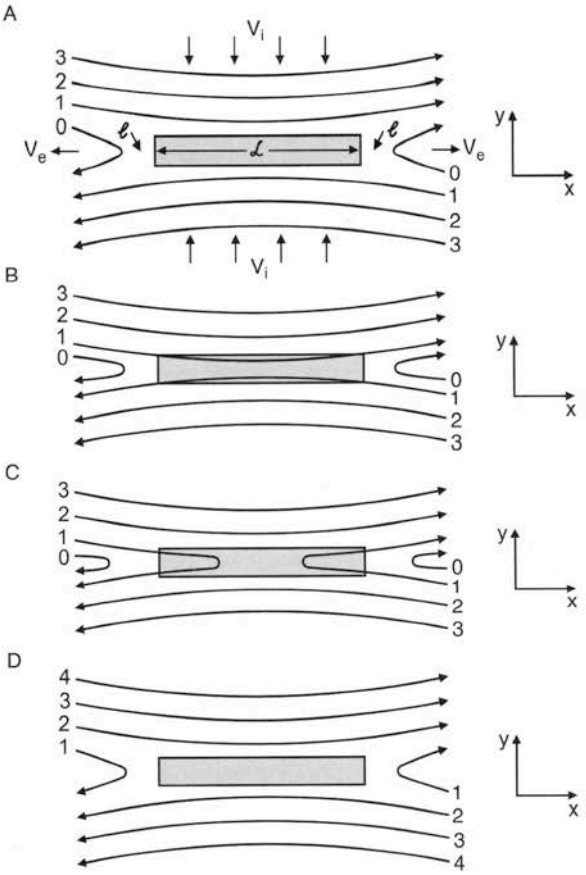

FIGURE 10 The Sweet–Parker reconnection mechanism. (A) Reconnection occurs when fluid motion brings slabs of oppositely directed magnetic fields together. The slabs have length $\mathscr{L}$ and velocity V_i. Pushing the slabs of field together creates a current sheet of thickness ℓ and ejects fluid at velocity V_e. The field lines labeled 1–3 approach the current sheet and field line 0 leaves it. (B) Field lines 1 enter the current sheet. (C) Field lines 1 are reconnected in the current sheet. (D) Field lines 1 leave the current sheet and move away in the $\pm x$ directions with velocity V_e. The configuration of field lines is now identical to that in A, but field lines n take the place of field lines n–1. Reconnection has changed the field line topology and dissipated magnetic energy.

shaded) of x width $\mathscr{L}$ and y width ℓ; it is assumed that ℓ is so much smaller than $\mathscr{L}$ that it is almost a current sheet. A steady inflow, V_i, in the $\pm y$ directions forces together two slabs of oppositely directed field $\pm B$ (Fig. 10A). The fluid is incompressible so that fluid must be ejected, with velocity V_e in the $\pm x$ directions. Figure 10B shows the field lines, labeled 1, moving into the reconnection region, and Fig. 10C shows them moving out after they have been reconnected. Their curvature implies a tension that assists the ejection of fluid in the $\pm x$ directions.

The object now is to determine V_i, V_e, and ℓ, assuming that the configuration is in a steady state

and that the Lundquist number $Lu = V_A \mathscr{L}/\eta$ is large. The argument rests on three simple balance laws:

1. Balance of fluid mass flowing into the reconnection layer with that flowing out: This gives $V\mathscr{L} = V_e \ell$.

2. Balance of fluid momentum in the reconnection layer. Since the flow in the reconnection layer is approximately one dimensional, it is governed by Bernoulli's law, which states that the sum of the total pressure P and the dynamic pressure $\frac{1}{2}\rho V^2$ is constant. Furthermore, the total pressure P is, in turn, the sum of the thermal pressure p and the magnetic pressure $p_M = \mathbf{B}^2/2\mu_0$. The sum, $S \equiv p + \mathbf{B}^2/2\mu_0 + \frac{1}{2}\rho V^2$, is therefore constant throughout the layer. By symmetry, the center of the configuration is a stagnation point ($\mathbf{V} = 0$), and at the midpoints on the long sides of the reconnection layer $\mathbf{V}$ is negligibly small so that $S \approx p + B^2/2\mu_0$. Outside the layer (i.e., for $|x| \gg \mathscr{L}$), the magnetic field is small so that at the ends of the layer where fluid is ejected in the $\pm x$ directions, $S \approx p + \frac{1}{2}\rho V_e^2$. Equating these two expressions for S shows that the ejection velocity is simply the Alfvén velocity: $V_e = V_A$.

3. Balance of magnetic energy: In the steady state, the influx of magnetic energy to the layer must equal the rate of ohmic dissipation in the layer. The influx rate is simply $(2V\mathscr{L})B^2/2\mu_0$ since the efflux from the narrow side edges of the reconnection region is negligible. The rate of ohmic dissipation is $(\mathscr{L}\ell)J^2/\sigma$, where by Ampère's law, $J = B/\mu_0\ell$. Since $\eta = 1/\mu_0\sigma$, the inflow velocity is related to the layer thickness by $V = \eta/\ell$.

Taken together, these three demands imply that

1. Since $Lu \gg 1$, the reconnection velocity, $V = V_A/\sqrt{Lu}$, is much smaller than V_A. It is proportional to a fractional power of the resistivity of the system; the growth rate of the tearing mode (discussed in Section 5) shows a similar fractional dependence.

2. The aspect ratio, $\ell/\mathscr{L}$, of the reconnection region is small, of order $Lu^{-1/2} \ll 1$. The direction of the merging fields imposes this anisotropy. It is consistent with the idea that magnetic energy is dissipated in a thin current sheet. Of course, the simultaneous smallness of V/V_A and the aspect ratio $\ell/\mathscr{L}$ is a consequence of their equality, by the balance law, and of the assumption $Lu \gg 1$.

Although conceptually simple and plausible, SPR tells a rather pessimistic story, namely that reconnection is a relatively slow process (i.e., $V = V_A/\sqrt{Lu} \ll V_A$, where $Lu \gg 1$ in cases of greatest interest). Many physical phenomena appear to require, for their explanation, fast reconnection (i.e., reconnection on ideal timescales or, equivalently, at Alfvénic velocities $V \sim V_A$). This is especially true of many solar and astrophysical phenomena, such as solar flares. The physics of fast reconnection is an active area of research in MHD and plasma physics.

Two main routes to fast reconnection have been proposed. Within the framework of MHD, one originally proposed by Petschek suggests that shock waves carry energy away from the reconnection layer. This rapid process of energy removal is thought to increase both the aspect ratio of the reconnection region and the reconnection rate. The Petschek mechanism predicts a reconnection velocity of order V_A, with only a weak logarithmic dependence on Lu [i.e., $V \sim V_A/\ln(Lu)$]. The alternate route to fast reconnection appeals to small-scale, non ideal, or kinetic processes that cannot be studied using the one-fluid model of MHD. All models of fast reconnection are controversial and they will evolve considerably in the years ahead.

4.3 MHD Turbulence

Many fluid systems are turbulent. This fact presents formidable obstacles to theorists and is likely to embarrass them for the foreseeable future. The motions and fields of a turbulent fluid have many length and timescales. In the classical picture of turbulence, these range from macroscales, $\mathscr{L}_{\text{macro}}$ and $\mathscr{T}_{\text{macro}}$, corresponding to scales on which the fluid is stirred, to dissipation scales, $\mathscr{L}_{\text{diss}}$ and $\mathscr{T}_{\text{diss}}$, which are dominated by viscosity. It is argued that $\mathscr{L}_{\text{macro}}/\mathscr{L}_{\text{diss}} \sim (Re)^{3/4}$, where $Re = \mathscr{V}_{\text{macro}}\mathscr{L}_{\text{macro}}/\nu$ is the Reynolds number. This is typically greater than 10^4, so the range of scales spans many decades and cannot be adequately resolved even by modern, high-speed computers.

In classic turbulence, interscale interaction occurs via a process of cascade in which larger eddies (i.e., fluctuations that have the appearance of vortical whorls) fragment into smaller eddies, thus producing a range of fluctuations on scales from $\mathscr{L}_{\text{macro}}$ to $\mathscr{L}_{\text{diss}}$. This process is encapsulated by a well-known parody by Louis Fry Richardson of a verse of Jonathan Swift:

> *Big whorls have little whorls, that feed on their velocity.*
> *And little whorls have lesser whorls, and so on to viscosity.*

In contrast to ordinary fluid turbulence, which can be thought of as a soup of eddies, MHD turbulence consists of a mixture of eddies and small-scale Alfvén

waves and is controlled by viscosity and resistivity. Thus, although the idea of a cascade remains useful for describing MHD turbulence, the interaction processes in MHD are considerably more complex than in nonmagnetic fluids. Perhaps the most important difference is that, since MHD turbulence involves Alfvén waves, it necessarily retains an element of memory or reversibility. Here, Alfvénic memory refers to the tendency of even small-scale magnetic fields (which are always present when Rm is large) to convert the energy in eddies (which cascades irreversibly) to reversible nondiffusive Alfvén wave motion. This is a consequence of the fact that wave motion is necessarily periodic and involves a restoring force.

Despite the difficulties discussed previously, there is considerable effort in the research community directed at numerical simulation of MHD turbulence. The large scales can be resolved numerically in so-called large eddy simulations (LES), but only if the effects of the unresolvable or subgrid scales (SGS) on the large scales are parameterized in some way. One popular, although controversial, expedient originated from an idea by Osborne Reynolds in the 19th century. He drew an analogy between the diffusive effects of the small-scale eddies and collisional diffusion processes at the molecular level. This suggested that the SGS similarly spread out the large-scale motions and fields diffusively, but on timescales $\tau_{\nu/\text{turb}} = \mathscr{L}^2/\nu_{\text{turb}}$ and $\tau_{\eta/\text{turb}} = \mathscr{L}^2/\eta_{\text{turb}}$ determined by turbulent diffusivities, ν_{turb} and η_{turb}, of order $\mathscr{L}_{\text{eddy}}\mathscr{V}_{\text{eddy}}$ that might be very large compared with the corresponding molecular values, ν_{mol} and η_{mol}.

Reynolds's idea is not totally satisfactory but is qualitatively useful. For example, the fact that $\eta_{\text{turb}} \gg \eta_{\text{mol}}$ in the solar convection zone explains, in a rough and ready way, why the timescale $\mathscr{T}$ of magnetic activity on the sun, as estimated by the period of the solar cycle, is on the order of a decade, even though $\tau_{\eta/\text{mol}}$ exceeds the age of the sun: $\mathscr{T}$ is determined by η_{turb} and not η_{mol} so that $\mathscr{T} \approx \tau_{\eta/\text{turb}}$.

Reynolds's idea also correctly implies that turbulence enhances viscous and ohmic dissipation. Although the magnetic Reynolds number Rm may be large when defined from $\mathscr{L}_{\text{macro}}$ and $\mathscr{V}_{\text{macro}}$, it may be small when $\mathscr{L}_{\text{eddy}}$ and $\mathscr{V}_{\text{eddy}}$ are used instead. Even if the characteristic macroscale field, $\mathscr{B}_{\text{macro}}$, is large compared with the typical eddy field, $\mathscr{B}_{\text{eddy}}$, so that the magnetic energy resides mostly in the macroscales, the magnetic energy may be dissipated mainly by the eddies. This is because $\mathscr{L}_{\text{eddy}} \ll \mathscr{L}_{\text{macro}}$ so that $\mathscr{J}_{\text{macro}} = \mathrm{O}(\mathscr{B}_{\text{macro}}/\mu_0\mathscr{L}_{\text{macro}})$ may be smaller than $\mathscr{J}_{\text{eddy}} = \mathrm{O}(\mathscr{B}_{\text{eddy}}/\mu_0\mathscr{L}_{\text{eddy}})$, even though $\mathscr{B}_{\text{eddy}} \ll \mathscr{B}_{\text{macro}}$. In many situations however, $\mathscr{B}_{\text{eddy}} \gg \mathscr{B}_{\text{macro}}$ so that the eddies contain most of the magnetic energy and are mainly responsible for its dissipation. Similarly, they may contain the majority of the kinetic energy and be the main cause of its viscous dissipation. The reader is cautioned, however, that the expressions for ν_{turb} and η_{turb} given here are estimates only. In particular, it has been appreciated that the Alfvénic memory intrinsic to MHD turbulence may cause significant reductions in ν_{turb} and η_{turb} in comparison with the estimates given here. The self-consistent calculations of ν_{turb} and η_{turb} are active topics of current research in MHD.

MHD propulsion and drag reduction are topics of considerable interest and usually concern systems for which $Rm \gg 1$ and in which MHD turbulence occurs. An extensive discussion of these topics is beyond the scope of this article.

4.4 Buoyancy in MHD

A real (nonideal) fluid has a nonzero thermal conductivity, K. The appropriate measure of the resulting conduction of heat is the thermal diffusivity, $\kappa = K/\rho C_p$, where C_p is the specific heat at constant pressure; the thermal diffusion time is $\tau_\kappa = \mathscr{L}^2/\kappa$. The finiteness of κ gives rise to the magnetic buoyancy of flux tubes. Such tubes are created by, for example, the turbulent motions in a stellar convection zone, such as that of the sun. These cause the prevailing magnetic field to become intermittent, with regions of strong field (i.e., flux ropes) being surrounded by regions of comparatively weak field. During a time $t \ll \tau_\eta$ after its formation, flux loss from a tube can be ignored. Radiative transport of heat, however, is very effective in a star and $\tau_\kappa \ll \tau_\eta$. Any difference in temperature between the rope and its surroundings diffuses away in a time of order τ_κ. It is reasonable to suppose that in the time interval $\tau_\kappa \ll t \ll \tau_\eta$, the temperature of the rope is the same as its surroundings but that the field B in the interior of the rope differs from the field $B_0 (< B)$ outside it. Magnetostatic balance requires that the total pressure exerted by the rope on its surroundings is approximately the same as the total pressure the surroundings exert on it: $p + B^2/2\mu_0 = p_0 + B_0^2/2\mu_0$. This means that the kinetic pressure p of the gas in the tube is less than that of its surroundings, p_0. However, since its temperature is the same, its density must be less. The tube is therefore buoyant and rises toward the stellar surface.

When the tube breaks through the stellar surface, dark regions occur that are called starspots (or sunspots in the case of the sun). That these spots are dark is another illustration of the constraining effects of the field. Near the stellar surface, heat is carried outward mainly by convective overturning, which within a tube is coupled to Alfvén waves that radiate energy and therefore tend to suppress the convective motions. The emerging heat therefore has to find a route that goes around the spots rather than through them. The spots are thus cooler and darker than their surroundings.

4.5 Amplification of Magnetic Fields in MHD

A magnetic field threading a sphere of solid iron of radius 1 m would disappear in approximately 1 s unless maintained by external current-carrying coils. Since $\tau_\eta \propto \mathscr{L}^2$, larger bodies can retain their fields longer, but many celestial bodies (planets, stars, galaxies, etc.) are magnetic and are believed to have been magnetic for times long compared with their magnetic diffusion times. The age of the geomagnetic field, for instance, exceeds 3×10^9 years, even though τ_η is less than 10^5 years. A process must exist that replenishes these fields as they diffuse from the conductor. This process is the same as that operating in commercial power stations: self-excited dynamo action. From a field $\mathbf{B}$, fluid motion creates the electromotive force (emf) $\mathbf{V} \times \mathbf{B}$ that generates the electric currents $\mathbf{J}$ necessary to create, by Ampère's law, $\mathbf{B}$.

Although it was stated previously that in turbulent flow eddies may be responsible for greatly enhancing diffusion of the large-scale part, $\mathbf{B}_{\text{macro}}$, of $\mathbf{B}$, these small-scale motions can, if they lack mirror symmetry, also act to replace the lost flux. The simplest manifestations of such symmetry breaking are helical motions. Helicity is defined as $\mathbf{V} \cdot \boldsymbol{\omega}$ where $\boldsymbol{\omega}$ is the vorticity of the flow, a vector that has Cartesian components $\partial V_z/\partial y - \partial V_y/\partial z$, $\partial V_x/\partial z - \partial V_z/\partial x$, $\partial V_y/\partial x - \partial V_x/\partial y$ and that is often written as curl$\mathbf{V}$ or $\nabla \times \mathbf{V}$. Helicity is a measure of how mirror symmetric the flow is; like a common carpenter's screw, a helical flow does not look the same when viewed in a mirror. Helicity is created naturally by the rotation of large systems such as the solar convection zone, where the rising and falling motions created by buoyancy acquire vertical vorticity through the action of the Coriolis force. Small-scale helical motions create a large-scale emf that, in the simplest case, is proportional to $\mathbf{B}_{\text{macro}}$ and is conventionally written $\alpha \mathbf{B}_{\text{macro}}$. This α effect may suffice to maintain $\mathbf{B}_{\text{macro}}$ and hence $\mathbf{B}_{\text{turb}}$ as well, thus creating a turbulent dynamo. The α effect is the cornerstone of a subject now called mean field electrodynamics. (Confusingly, this is often known by the acronym MFE, which we reserved as an abbreviation for magnetic fusion energy.)

The α effect illustrates the danger, mentioned previously, of adopting the Reynolds ansatz too uncritically; through their anisotropy and lack of mirror symmetry, small-scale motions can create large-scale emfs that are not recognized when η_{mol} is merely replaced by η_{turb}. It should also be mentioned that the issue of Alfvénic memory appears once again in the context of the dynamo and the α effect. Recent research has suggested that because of memory effects and constraints on the rate of magnetic reconnection, the α effect at large Rm may be much weaker than it would be were the dynamical effects of the small-scale eddies ignored, as was done in the early days of mean field theory. Further developments in this important research area may be expected in the near future.

The interested reader can get an intuitive, hands-on perspective on a particular type of dynamo process by the following home demonstration, which also illustrates several of the processes described in this section and the last. Obtain an elastic (rubber) band. This loosely corresponds to the flux tube in Fig. 11A, its tension being the sum of the tensions in the magnetic field lines it contains (i.e., it is proportional to the energy of the field within it).

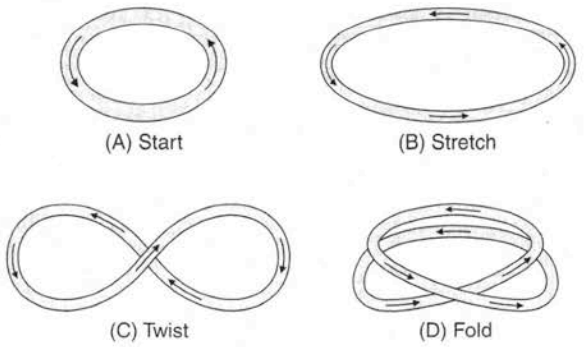

FIGURE 11 The stretch–twist–fold dynamo. (A) The initial undeformed flux tube; (B) the result of stretching it to twice its length; (C) the stretched tube is twisted into the shape of an infinity sign ∞; and (D) the result of folding one loop of the ∞ over onto the other. Reconnection in D can produce two loops of the same size as the initial tube.

The tension in the band may be systematically increased by a three-step, stretch–twist–fold process:

1. Stretch the rubber band to double its length.
2. Twist it into the shape of an infinity sign, ∞.
3. Fold the loops on top of one another to form two linked loops of the same size as the original band.

These steps are illustrated in Fig. 11B–D. In a similar way to the rubber band, the energy within and the tension of the flux tube are increased by a factor of 4. This is the essence of a dynamo, the creation of magnetic energy by helical motion.

In principle, these steps can be repeated over and over again, with the sense of twist in step 2 being always the same. This gives the band the sense of handedness of a screw motion and the broken reflection symmetry and helical motion that are crucial to the success of the dynamo. The tension in the band (analogous to the magnetic tension) increases progressively as the steps are repeated, and at some stage the reader's hands will tire, making it impossible to increase the tension further. This illustrates the end of the kinematic regime (in which fluid motion is prescribed *a priori* and the field grows) and the beginning of the dynamic regime (in which the field quenches its own further growth). If the reader lets go of the band at any stage, it will immediately relax back to its initial state. This illustrates the crucial importance of magnetic reconnection as a means of locking in the amplified magnetic field. In other words, magnetic reconnection provides the crucial element of irreversibility in the dynamo. The analogue of magnetic reconnection in the case of the rubber band could be achieved by fusing the two loops together after the stretch–twist–fold process.

In recent years, much effort has been expended on the study of fast dynamos, which are defined as processes of field amplification that operates on timescales independent of τ_η in systems with $Rm \gg 1$. It should be apparent to the reader that a fast dynamo necessarily requires fast reconnection in order to lock in the dynamo-generated field. Thus, the problems of fast reconnection and those of the fast dynamo are intimately linked.

4.6 Magnetic Helicity and Relaxation in MHD

No doubt the reader has noticed that the past three sections, which discuss magnetic reconnection, turbulent transport of magnetic fields, and the dynamo process, all concern the following broader question: Given certain initial conditions, what magnetic configuration does the magnetofluid ultimately adopt? This question seeks to identify the final state when some very complex dynamical processes, involving the dissipative phenomena mentioned previously (as well others, some unknown), are at work.

Apart from a very few simple, exactly soluble cases (that nearly always have an unrealistically high degree of symmetry built in), there are two main ways of finding the final state.

The first is to integrate the MHD equations directly using a computer. This approach forces the researcher to confront all the thorny issues of MHD turbulence, SGS modeling, etc. described previously. Moreover, such brute force tactics are often expensive and inefficient. One is naturally motivated to seek other approaches that are bolder but simpler. Foremost among these is constrained relaxation. This variational method seeks to identify the final state as one that minimizes the magnetic energy, subject to certain constraints. The central issue then becomes the identification and inclusion of the most important constraint or constraints.

A natural candidate for consideration as a constraint is the magnetic helicity. This is the analogue of the (kinetic) helicity, which was previously defined as $\mathbf{V} \cdot \boldsymbol{\omega}$, where $\boldsymbol{\omega} = \mathrm{curl}\mathbf{V}$. Conversely, $\mathbf{V}$ can be derived from $\boldsymbol{\omega}$ by integration in an uncurling operation. Likewise, a vector $\mathbf{A}$ can be obtained from $\mathbf{B}$ by a similar uncurling operation. This defines a vector potential, $\mathbf{A}$. The scalar product $K = \mathbf{A} \cdot \mathbf{B}$ is the magnetic helicity. It is conserved in the motion of an ideal fluid, and this is why it is significant in MHD. Physically, magnetic helicity quantifies the self-linkage or knottedness of the magnetic field lines and is thus a measure of the topological complexity of the field. Indeed, the invariance of field line topology in ideal MHD is the origin of the conservation of magnetic helicity.

If an MSE is analyzed using ideal MHD, it is found that magnetic helicity is conserved in detail in the sense that if we regard the MSE as an assembly of infinitesimally thin flux tubes of volume Δv and labeled by parameters α and β, their individual magnetic helicities, $K_{\alpha,\beta} = (\mathbf{A} \cdot \mathbf{B})_{\alpha,\beta} \Delta v$, are conserved, although they are not the same for each tube. If instead nonideal MHD is used in analyzing the MSE, the configuration will relax toward its final state on a timescale determined by the resistivity and other slow diffusion mechanisms. In this process,

individual flux tubes lose their identity through magnetic diffusion and turbulent cascade. Thus, the local magnetic helicity, $K_{\alpha,\beta}$, associated with a given thin flux tube, is *not* conserved. However, J. B. Taylor made the insightful conjecture that the global magnetic helicity (i.e., the sum of $K_{\alpha,\beta}$ over the system) would be approximately conserved on the timescale of the relaxation.

Global helicity is the integral of K over the entire system. It is, in some sense, a coarse-grained topological invariant that is also related to the self-inductance of the plasma. Taylor relaxation theory proposes to determine relaxed states by minimizing magnetic energy subject to the constraint of constant global magnetic helicity. The resulting Taylor states have the property that the current is linearly proportional to the field (i.e., $\mathbf{J}=\lambda\mathbf{B}$, where λ is a constant). This, is a force-free field of the special type described in Section 3 for which the component, $J_{\|}$, of $\mathbf{J}$ parallel to $\mathbf{B}$ is everywhere the same. In Section 5.3.2, we discuss kink-tearing instabilities of toroidal MSE. These instabilities are current driven (i.e., they exist only because $\nabla J_{\|}$ is nonzero). Since $\nabla J_{\|}=0$ in the Taylor relaxed state, it is stable to kink-tearing modes.

Taylor relaxation theory has been very successful in explaining the relaxed mean field profiles of low β confined plasmas, especially the reversed field pinch (RFP) and spheromak. Of particular note is Taylor's successful prediction of the F–Θ curve for the RFP. The F–Θ curve relates the degree of field reversal to the poloidal field at the edge of the RFP and is an experimentally derived signature of the final RFP state. In relation to Section 4.4, it is worth noting that the relaxed state is maintained by a cyclic dynamo process in which dissipative excursions from the Taylor state trigger instabilities that drive the plasma back to relaxed state.

The main mystery of Taylor relaxation theory is why it works so well. In other words, why is the global helicity the most important constraint on turbulent relaxation? There are at least three plausible answers:

1. *Enhanced dissipation:* Turbulence and dissipation drive magnetic reconnection, which destroys domains of local magnetic helicity on all but the largest scale. Thus, as the system evolves, the global magnetic helicity is the only surviving topological invariant.

2. *Field line stochasticity:* In the initial state of the configuration, the field lines lie on magnetic surfaces, each labeled by its hydrostatic pressure p. However, as the configuration relaxes to the force-free state of constant p, the identity of the surfaces evanesces, and field lines become increasingly stochastic. Ultimately, as the turbulent relaxation proceeds, the entire MSE is threaded by a single field line. Since magnetic helicity is calculated by volume integration over a region enclosed by a magnetic surface, and all other magnetic surfaces are destroyed, only global magnetic helicity is relevant to a stochastic state.

3. *Selective decay:* In three-dimensional MHD turbulence, energy cascades to small scales. It can be shown, however, that magnetic helicity cascades inversely to large scales. As a result, magnetic helicity accumulates on the largest scales of the system, with minimal coupling to dissipation. Thus, magnetic helicity is dynamically rugged, whereas energy decays.

It should be noted that these are only plausibility arguments, and that a rigorous justification of the Taylor hypothesis remains an elusive goal of current research.

5. STABILITY OF MAGNETICALLY CONFINED PLASMAS

5.1 Generic Issues

Configurations of MHD fluids are analyzed using the concepts of equilibrium and stability. These are used to classify a variety of possible configurations according to their intrinsic interest, potential utility, importance for science and technology, and so forth. They are vital in the context of magnetic plasma confinement for the success of controlled fusion (hereafter referred to as MFE). This is the only application considered here, but there are many others in astrophysics, geophysics, space plasma dynamics, and MHD power generation.

MHD equilibria are configurations in which the plasma pressure gradient, ∇p, balances the $\mathbf{J}\times\mathbf{B}$ force (Lorentz force) and any other body forces acting on the magnetofluid. An equilibrium in which the balance is dominated by the pressure gradient and the Lorentz force is referred to as a *MSE*. All equilibria of interest in the context of MFE are MSEs. In general, the magnetic fields in MSEs are produced in part by external coils and in part by plasma currents. They are characterized by the pressure and current profiles $p(r, \theta, \phi)$ and $\mathbf{J}(r, \theta, \phi)$. In toroidal MSEs, these are independent of ϕ, the angle around the torus in the toroidal

direction, but still depend on θ, the angle that increases in the so-called poloidal direction.

Interesting MSEs almost always have closed magnetic flux surfaces (i.e., surfaces that enclose a specified amount of magnetic flux). These are labeled by an effective radius r, and because they are so significant, we generally suppress the dependence of p and $\mathbf{J}$ on θ and ϕ. Charged particles in a plasma cannot readily cross a flux surface and are therefore confined. For this reason, an MSE is sometimes called a magnetic bottle.

MSEs have a high degree of symmetry, corresponding to closed toroidal, spheroidal, or helical configurations. Toroidal MSEs of interest in the context of MFE include the tokamak (based on a Russian acronym for maximum current) and the RFP. Together, these two configurations are referred to as toroidal pinches since plasma is confined by a toroidal current that produces a magnetic field, which in turn acts to pinch the plasma column. A tokamak has a strong, externally applied toroidal magnetic field, whereas a RFP plasma generates its own toroidal field by a process of constrained relaxation, whereby some of the toroidal current is dynamically twisted into the poloidal direction. This relaxation process is closely related to that of the dynamo described previously. RFPs are intrinsically dynamic (i.e., not quiescent) in nature. Spheroidal MSEs include the spheromak and the spherical torus, whereas helical MSEs include the heliac, a type of stellarator. Stellarator MSEs do not rely on inductively driven currents as do toroidal pinches, but they sacrifice the virtues of toroidal symmetry. In this section, the discussion is limited for reasons of brevity and clarity to toroidal pinches in general, and tokamaks in particular. The MSE of a tokamak is particularly simple in that the pressure and toroidal current profiles, $p = p(R)$ and $J_\phi = J_\phi(R)$, can be parameterized by a single coordinate, R, that may be thought of as a (generalized) distance from the symmetry axis.

Once the existence of a closed MSE is established, the next question is whether it is magnetohydrodynamically stable—that is, whether initial, small perturbations that break the symmetry of the equilibrium tend to reinforce themselves and grow. This growth is due to the release of potential energy stored in the initial MSE and is accompanied by a relaxation of the pressure and/or current profiles $p(r)$ and $J_\phi(r)$, which tends to lower the initial potential energy and degrade the quality of the nascent MSE. Instability is a linear concept and is relevant for only a few growth times (at most), until the dynamics enter the nonlinear regime, characterized by finite (i.e., not small) amplitude perturbations. Instabilities saturate (i.e., cease growing) either when the plasma arrives at a new secondary equilibrium, which is a MSE with lower potential energy than the initial equilibrium, in which the symmetry is usually broken as well, or when the kinetic energy of the plasma motion is lost through dissipation (e.g., through viscosity). The latter often occurs as a consequence of the cascade to small scales characteristic of MHD turbulence.

MHD instabilities are usually classified as either pressure driven [when they are associated with relaxation of $p(r)$] or current driven [when associated with relaxation of $J_\phi(r)$]. They are either ideal or resistive. Ideal instabilities occur without a violation of Alfvén's frozen flux constraint, whereas resistive instabilities require some decoupling of field and fluid, usually by collisional resistivity, to trigger the energy-release process. MHD instabilities are of great interest in the context of MFE, because they limit the class of viable MSEs and thus severely constrain the performance of magnetic fusion devices.

Entire books have been devoted to the MHD stability of confinement devices for MFE. There is space here to describe only a few of the basic concepts and their application to MFE. One way of investigating dynamical stability makes use of the fact that ideal MHD conserves the total energy E of the system. This is the sum of the kinetic energy E_K, the magnetic energy E_M, and the internal energy of the plasma, E_I. Before perturbation, $\mathbf{V} = 0$ and therefore $E_K = 0$ so that $E = E_M + E_I$. The perturbation creates a small initial E_K and this may grow at the expense of $E_M + E_I$, indicating that the initial state is unstable; if the initial state is linearly stable, E_K remains small.

The situation may be described conceptually by analogy with a ball rolling under gravity on a surface S. Then E_K is the kinetic energy of the ball and its height z above some reference level plays the role of $E_M + E_I$. A magnetostatic equilibrium is analogous to the ball being at rest at some point P where the surface is level (i.e., where the tangent plane at P to S is horizontal, as at the points indicated in Fig. 12). In Fig. 12A, the ball rests at a global minimum of z, and the system is not only linearly stable but also globally stable (i.e., stable to all perturbations no matter how large they are or in which horizontal direction they occur). In Fig. 12B, the ball is at an unstable equilibrium that is destroyed if perturbed in any horizontal direction. Figure 12C also illustrates an unstable state; although it is true that some

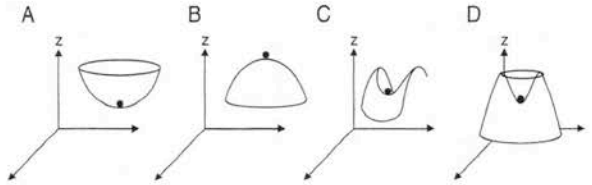

FIGURE 12 Equilibrium points (•) of a ball rolling on a surface. (A) global stability; (B) instability at a maximum of z; (C) instability at a saddle point of z; (D) stability for small perturbations but not large.

perturbations increase z (suggesting stability), other directions of perturbation exist that will cause the ball to descend permanently from the saddle point. In Fig. 12D, a sufficiently large perturbation will take the ball over an adjacent hill, after which it descends permanently to a state remote from its starting point (i.e., the initial state is linearly stable but unstable to finite amplitude perturbations).

Similarly, if $E_M + E_I$ increases for every small perturbation of a MSE, it is linearly stable, as in Figs 12A and 12D. The MSE is unstable if any perturbation exists that reduces $E_M + E_I$, as in Figs 12B and 12C. Figure 12C is the better analogue for a MSE since many directions of perturbation do not threaten a MSE; perturbations that bend field lines increase E_M and those that compress the plasma increase both E_M and E_I. Other directions of perturbation, however, may exist that reduce $E_M + E_I$, and these are the perturbations that should be understood and, as far as possible, eliminated. These directions are usually associated with perturbations that relax the current or pressure gradients.

5.2 Magnetically Confined Plasmas and MFE

The hope of controlling the release of thermonuclear energy by the fusion of light nuclei provides a very powerful incentive for the study of plasma physics and MHD. To make light nuclei react and release energy, they must be forced together against their mutual electrostatic repulsion. This happens naturally at the enormous pressures characteristic of the interiors of stars, such as the sun. The aim of MFE, of course, is to create high plasma pressure MSEs using magnetic fields. The efficiency of the MSE is determined (in part) by the dimensionless parameter β, (which is the ratio of the plasma pressure p to the magnetic pressure $B^2/2\mu_0$. For fusion to occur, high pressure must be sustained long enough for the ignited plasma to replace its energy, via the fusion burn, faster than it loses it through leakage of energy across the confining fields. Thus, both high plasma pressure and a sufficiently long plasma energy confinement time, τ_E, are necessary for the success of MFE. The Lawson criteria for ignition of a fusion burn are that the ion temperature T_i exceeds $4.5 \times 10^7 K$ and that the product of density and energy confinement time $n\tau_E \geq 10^{20}\,\mathrm{m}^{-3}\,\mathrm{s}$. These two conditions can be combined into a single criterion often referred to as the Lawson triple product. This requires that $nT\tau_E > 4.5 \times 10^{27}\,\mathrm{m}^{-3}\,\mathrm{Ks}$. This product is proportional to $\beta B^2 \tau_E$, indicating that high beta and large fields are desirable for fusion, assuming that τ_E does not degrade rapidly with either. In addition, high β is intrinsically desirable for economic reasons.

The required Lawson number is lower for a DT plasma than for a D plasma. Tritium, which is virtually nonexistent in nature, may be bred in a lithium blanket surrounding the ignited plasma in which alpha particles escaping from the burning DT plasma react to create T, which can subsequently be extracted to fuel the fusion reactions. Of course, the commercial viability of MFE demands even better performance. The fusion reactions occurring during confinement must recoup the cost of creating and heating the plasma and all other overheads of the system, such as collecting T from the lithium blanket and extracting the spent fuel from the reaction chamber. This necessarily raises the required Lawson triple product in comparison with the value needed for ignition. In practice, Lawson triple products in excess of $2.4 \times 10^{28}\,\mathrm{m}^{-3}\,\mathrm{K\,s}$ are thought to be required for a fusion power plant producing 1 GW of power.

The performance of a magnetic confinement device is determined by

1. *The magnetic configuration*: the external magnetic fields and plasma currents that together define the geometry of the MSE and the strength of the magnetic bottle. Today's tokamaks rely heavily on optimization of the magnetic geometry by shaping of the cross section to achieve peak performance.
2. *Heating power and method*: the means by which the plasma is heated. These include ohmic heating, neutral beam injection, radiofrequency heating, and self-heating by the slowing down of fusion-generated alpha particles. Most scenarios for achieving ignition require auxiliary (i.e., non-ohmic) heating, usually via injection of radiofrequency waves that resonate with a characteristic frequency (known as the cyclotron frequency) of a class of plasma particles.

3. *Fueling*: the means by which fuel is injected. These include gas-puffing, pellet injection, and beam fueling.

4. *Boundary control*: the means by which the deleterious effects of impurity accumulation and other undesirable consequences of plasma–wall interaction are minimized by control of the plasma boundary. This is usually accomplished by a special magnetic configuration called a divertor. This diverts plasma outside the confinement region to a separate chamber, where interaction with walls occurs.

5. *Momentum input*: the means, usually via neutral beam injection, whereby plasma rotation is generated. Toroidal rotation is desirable for optimizing energy confinement and controlling certain types of MHD instabilities.

The principal limitations on fusion plasma performance are

1. *Collisional transport*: There is an irreducible minimum to the cross-field losses, that is, for a given magnetic geometry, *some* losses through diffusion are due to collisions between charged particles (analogous to, but dynamically different from, molecular diffusion in fluids) and these are unavoidable.

2. *Radiative losses*, especially due to *impurities* in the plasma.

3. *Macroscopic MHD instabilities*: MHD instabilities are large-scale perturbations that constrain possible pressure and current profiles. Robust ideal instabilities set hard limits on $p(r)$, $\mathbf{J}(r)$, β, etc. that place an upper bound on the possible Lawson number. Resistive instabilities may set soft limits (i.e., bounds that can be exceeded but only at unacceptably high cost in, for example, heating power). Both ideal and resistive instabilities can lead to disruptions, which are catastrophic events that result in termination of the plasma discharge and may also damage the confinement vessel.

4. *Microinstabilities*: These are small-scale instabilities, driven by local temperature and density gradients, leading to small-scale turbulence that degrades energy and particle confinement through turbulent transport. Microinstabilities typically require a description in terms of two (or more) fluids or one using kinetic equations. Discussion of these is beyond the scope of this article. Microinstabilities typically produce cross-field leakage of energy and particles that far exceeds that due to collisions. They essentially control τ_E, which enters the Lawson triple product.

Instabilities are the key players that limit achievable Lawson numbers. MHD phenomena typically determine β and the plasma pressure p, whereas microinstabilities determine τ_E. Thus, the interplay of macro- and microinstabilities is a recurring theme in the design of MFE devices.

MHD instabilities have played a prominent role in the history of MFE, especially in elucidating the behavior of tokamaks. The early predictions of rapid progress in MFE relied on naive expectations based only on considerations of collisional and radiative losses. Fusion researchers soon learned, however, that an evil genie named instabilities lurked in the magnetic bottle and was only too anxious to escape. The instabilities it created were difficult to control. Thus, the hopes of the MFE pioneers were dashed by the struggle against unexpected, premature termination of discharges by disruptions created by MHD instabilities. The genie had to be persuaded to remain in the bottle. The instabilities had to be understood and minimized or eliminated.

Much, indeed most, research on tokamaks in the late 1960s and 1970s focused on current-driven instabilities called kink-tearing modes, which can disrupt the current profile and thus the discharge. The output of this phase of fusion research was a greatly improved understanding of the parameter space of viable tokamak operations, particularly with respect to current profile and magnetic field configurations. The emphasis of tokamak research in the 1980s and early to mid-1990s shifted to microinstabilities and the turbulent transport associated with them. The aim here, simply stated, was to understand and predict the parameter scaling of τ_E. Great progress was made.

A watershed in this line of research was reached with the discovery of spontaneously formed transport barriers at the edge of, and within, the plasma. A transport barrier is a localized region in which turbulence due to microinstabilities is greatly reduced or extinguished so that cross-field leakage declines to very low, collisional levels. This, in turn, results in the formation of regions of steep pressure gradient. Transport barriers usually form via a spontaneous transition to a state of strongly sheared poloidal and/or toroidal flow, which tears apart the eddies driven by microinstabilites before they can cause significant leakage. Present-day transport barriers can sustain temperature gradients that seem almost incredibly large, in excess of 1 million degrees per inch. Profiles with and without transport barriers are shown in Fig. 13.

The discovery and exploitation of transport barriers stimulated a renewed interest in MHD stability in the late 1990s, a trend that continues to

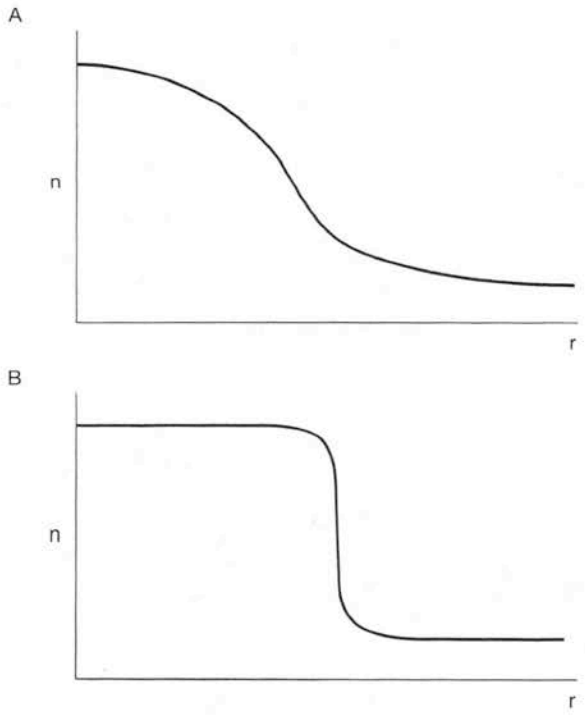

FIGURE 13 Profiles with and without transport barrier. (A) Normal profile; low confinement. (B) Profile with transport barrier; high confinement. Particle density is denoted by n.

this day. In confining the plasma better, a transport barrier also creates a larger pressure gradient in the plasma column that brings it closer to the verge of ideal MHD instability. In the jargon of MFE, enhanced confinement is necessary to reach the β limit. Thus, much of the current research on MFE is devoted to avoiding or mitigating the effects of pressure-driven ideal MHD instabilities via cross-section shaping, active feedback techniques, and profile control. Paradoxically, after 40 years of research on how to exterminate microinstabilities, effort is now being expended on finding ways to stimulate them at opportune times. The aim is to reap the full benefits of transport barriers by avoiding disruptions while at the same time controlling impurity accumulation.

5.3 Examples of MHD Instabilities in MFE Plasmas

As mentioned previously, the MHD instability of MFE plasmas is an exceptionally complex topic but is the subject of several excellent monographs. Here, we give only an introduction to the major pressure gradient and current gradient instability

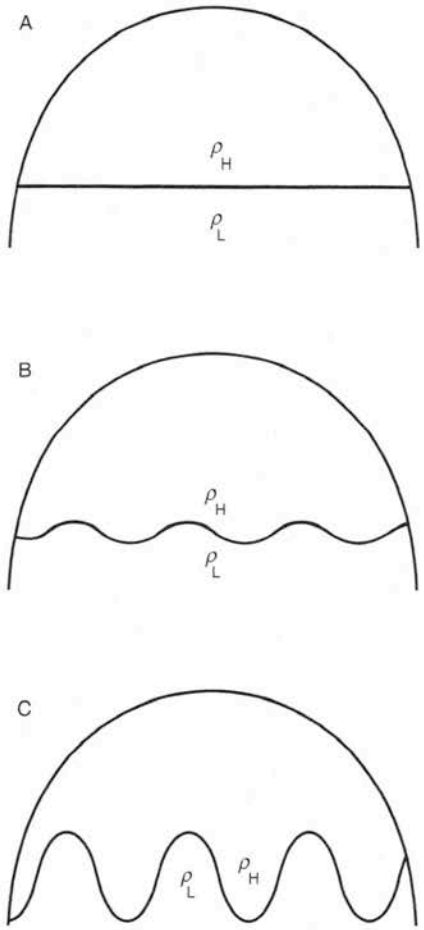

FIGURE 14 Development of Rayleigh–Taylor instability. (A) Initial equilibrium, with heavy fluid (density ρ_H) on top of light fluid (density ρ_L). (B) Ripples form on the interface. (C) Ripples are amplified by Rayleigh–Taylor instability.

mechanisms; interchange-ballooning modes and kink-tearing modes, respectively.

5.3.1 Interchange-Ballooning Modes

These modes, like all ideal MHD instabilities driven by the pressure gradient, are related to Rayleigh–Taylor instability, familiar from classical (nonmagnetic) fluid dynamics. Rayleigh–Taylor instability occurs when ripples are excited on the interface between a heavy fluid (e.g., water) sitting atop a lighter fluid (e.g., air) in a gravitational field, as shown in Fig. 14. Everyone knows what happens: The water falls out of the glass. What is not so apparent is that the initial configuration of the water and air is in equilibrium, but that the equilibrium is unstable to the growth of ripple perturbations. The experimentally inclined reader (with inexpensive carpeting) may easily convince himself or herself of

this by filling a glass to the brim, placing a strong piece of cardboard (preferably two-ply) over the surface of the water and in contact with the rim of the glass, and then inverting the glass. Because the presence of the cardboard prevents the formation of surface ripples, the water will not fall, so long as the integrity of the cardboard is maintained. Of course, the free energy source for this instability is simply the gravitational potential energy stored in the initial configuration (i.e., the elevated heavy fluid); the gradient that relaxes is simply the density gradient.

The analogue of the Rayleigh–Taylor instability in the MHD of magnetically confined plasmas is the interchange instability. Interchange instability relaxes the gradient in density, or more generally in the pressure gradient, by lowering the effective gravitational potential energy of the system. It does this by interchanging a tube of high-pressure fluid with a tube of low-pressure fluid, as shown in Fig. 15. In a magnetically confined plasma, the role of gravity is played by the centrifugal force exerted on the plasma particles as they traverse curved field lines. This results in a net body force that resembles a gravitational force. Thus, if field lines curve or sag away from regions of higher pressure, the system is interchange unstable, whereas if they curve or sag toward regions of higher pressure, the system is interchange stable (Fig. 16). Equivalently, an interchange stable system is said to have favorable curvature, whereas one that is unstable is said to have unfavorable curvature. Also, it is important to realize that the conceptual image of an interchange of two plasma tubes is motivated by the fact that potential energy release will be maximal when the perturbation does not spend any portion of its energy budget on bending field lines. In other words, a pure interchange instability does not couple to Alfvén waves. In reality, the physical appearance of an interchange instability resembles that of a convection roll (Fig. 17).

In magnetic confinement devices of practical interest (including tokamaks), the magnetic curvature is not constant but, rather, varies along the field lines. Interchange stability is then determined by an average of the magnetic curvature over the extent of the field line. One key virtue of the tokamak is that its configuration has favorable average curvature and thus is interchange stable. However, as one follows a field line around the tokamak, one traverses regions of locally unfavorable curvature on the outboard side of the torus and locally favorable curvature on the inboard side. Thus, if perturbations are larger and stronger in regions of locally unfavorable curvature

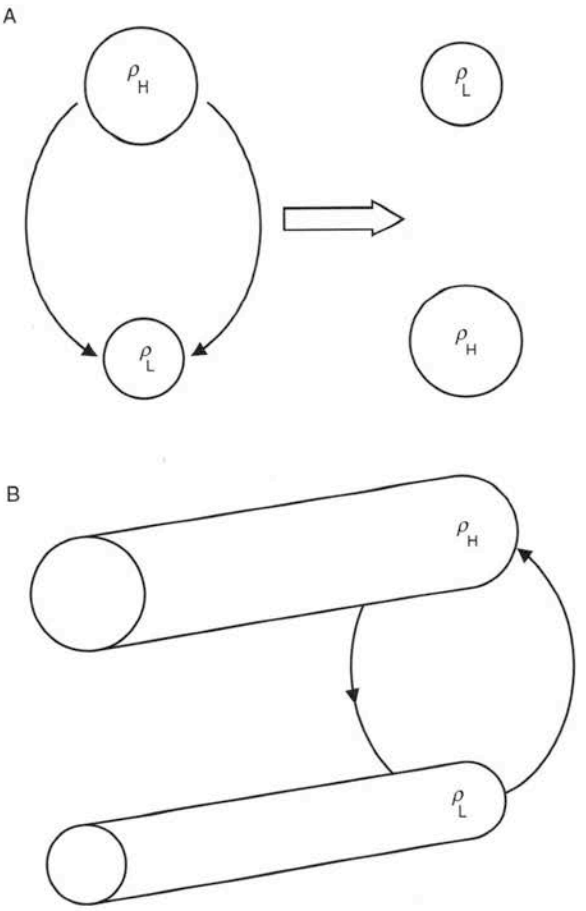

FIGURE 15 Interchange instability. (A) Interchange instability switches tubes of heavy and light fluid (densities ρ_H and ρ_L, respectively. (B) Oblique view of tube interchange; note that tubes, which are aligned with field lines, are not bent.

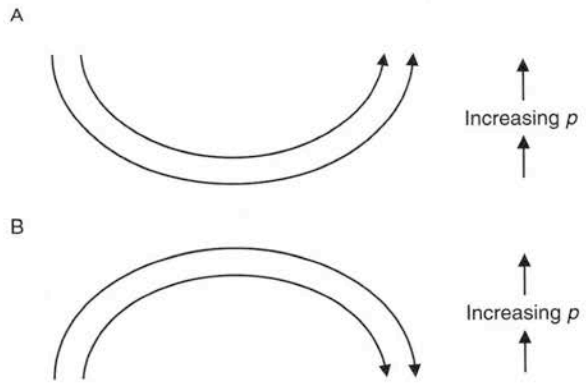

FIGURE 16 Favorable and unfavorable curvature. (A) Unfavorable curvature: Field lines sag away from the region of high pressure p. (B) Favorable curvature: Field lines curve toward the high-pressure region.

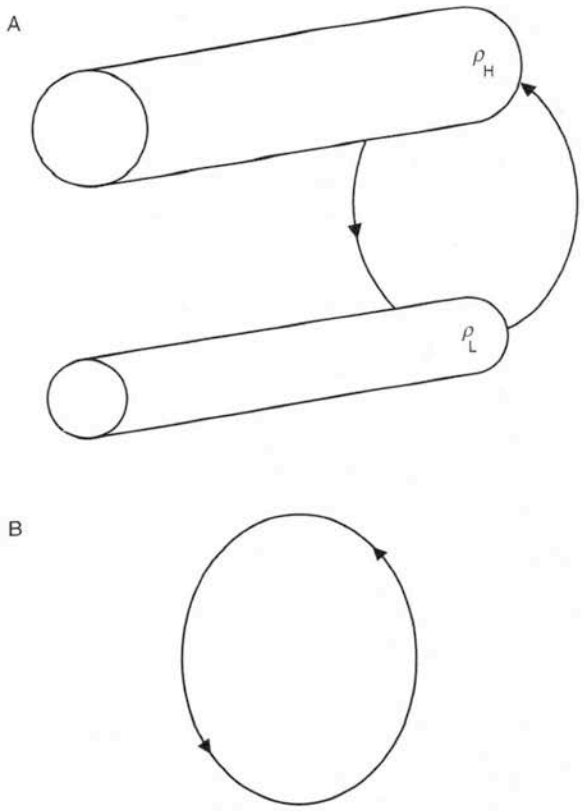

FIGURE 17 Depiction of an interchange convection roll; see legend to Fig. 15.

than they are in the locally favorable regions, instability is possible. These are called ballooning instabilities because the perturbation in the plasma pressure balloons the plasma outward in regions of unfavorable curvature. A physical picture of a ballooning instability may be gained by thinking of what happens when one overinflates a bicycle tire. Of course, the tire eventually ruptures. If there is no flaw in the tire material, the rupture will be likely to occur on the outboard portion of the wheel because the inboard portion is supported by the structural frame of the wheel and is thus mechanically more resilient. Indeed, sometimes an aneurysm will form in the tire. Finite-amplitude ballooning may be thought of as a kind of aneurysm in the magnetic surface that is driven by high plasma pressure interior to that surface. Finite-amplitude ballooning-kink instabilities are shown in Figs 18 and 19. Figure 18 shows development of the instability in a poloidal cross-section. Notice how fingers form on the outboard side of the torus. Figure 19 shows the magnetic flux surfaces. Notice how the ballooning instability produces crenelations in these.

Although ballooning instabilities are closely related to interchange instabilities, they differ crucially in that the perturbations vary along the field lines and therefore must bend the field lines. Thus, ballooning instabilities couple localized interchange motions to Alfvén waves. For ballooning instability to occur, the energy released by interchange motions in the unfavorable regions must exceed the energy expended in bending the magnetic field lines. Thus, there is a minimal or critical pressure gradient required for ballooning instability to occur. This is in sharp contrast to the interchange mode (in a system with a curvature that is on average unfavorable), which, in ideal MHD, can occur for any pressure gradient. The critical pressure gradient for ballooning instability plays a central role in the ultimate determination of the maximum achievable β for a specific configuration (i.e., its beta limit). In practice, the magnetic geometry and magnetic field strength determine the critical pressure gradient for ballooning instability. One important feature of magnetic geometry is the magnetic shear, which parameterizes how rapidly the direction of field lines changes as a function of radius r. Magnetic shear plays an important and subtle role in the detailed dynamics of ballooning instabilities. A complete discussion of this is beyond the scope of this article.

5.3.2 Kink-Tearing Modes

Kink-tearing modes are all driven by the current gradient, although the symptom of instability is often related to the pitch of the magnetic field lines. The physical nature of the modes is best illustrated by a sequential discussion of sausage instabilities, kink instabilities, and tearing instabilities.

Consider the Z pinch (Fig. 7A). Figure 20 illustrates a type of perturbation, sometimes called a sausage mode, which is axisymmetric around the axis of the pinch. The existence of the sausage mode of instability can be explained rather simply. As discussed in Section 2, the field B_θ outside the plasma column, created by a current I flowing down it, is azimuthal in direction and of strength $\mu_0 I/2\pi r$. On the surface of the column, the field strength is therefore $\mu_0 I/2\pi a$, where a is the local radius of the column, which varies when the tube is pinched. The pinched column then resembles a tube of sausage meat that has been compressed to create a chain of links. The surface field and the associated field line tension are greater where the column necks and smaller where it bulges. This is the field that confines the plasma column, and since I is constant, the tension it exerts on the necks of the chain further

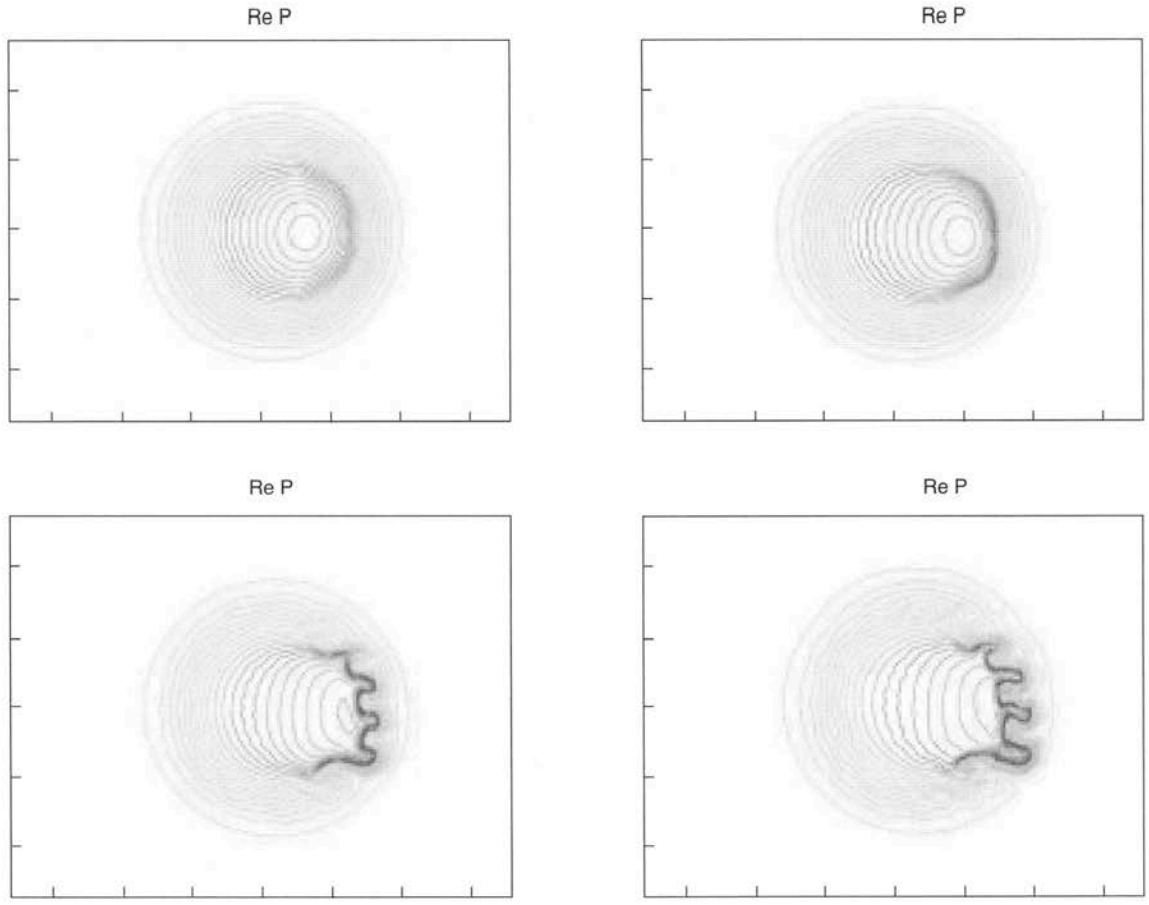

FIGURE 18 Development of a ballooning mode as seen in a poloidal cross section of the torus. The magnetic axis is on the left of each panel. The sequence of panels is as follows: top left, top right, bottom left, and bottom right. Note that perturbations are larger on the outboard midplane regions (on the right). Also note that as the perturbation grows, it evolves to form fingers or spikes. Courtesy of S. C. Jardin and the Center for Extended MHD Modeling, Princeton Plasma Physics Laboratory.

FIGURE 19 Development of a ballooning-kink mode in a torus. Note how a side view of the finger formation reveals the tendency of the ballooning mode to crenelate the plasma and break it into ribbons. Courtesy of S. C. Jardin and the Center for Extended MHD Modeling, Princeton Plasma Physics Laboratory.

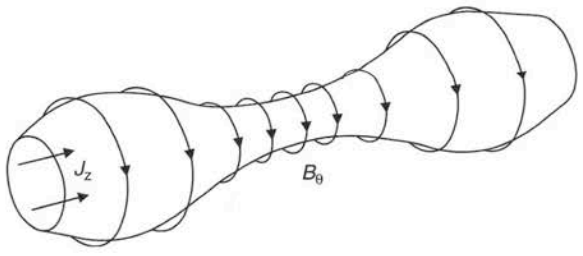

FIGURE 20 The sausage mode of instability of a Z pinch; lines of force encircling a current-carrying plasma column are shown. J_z indicates the cross section through which the current enters.

increases the initial deformation of the column. This self-reinforcing, positive feedback loop is indicative of an instability process that tends to break up the column into a chain of plasmoids (i.e., plasma droplets). For obvious reasons, the instability is called the sausage instability. The mechanism of sausage instability is closely related to that causing a thin stream of water from a faucet to break up into a

line of spheroidal droplets. In this case, surface tension plays the role of field line tension.

The sausage instability may be stabilized by an axial field B_z of sufficient strength within the column, which provides a tension that opposes the formation of necks. The critical strength of B_z necessary for stabilization can be estimated by comparing the field energy released by necking of the column with the energetic costs of deforming the axial field B_z. Because necking motions must conserve axial magnetic flux, the change, $\Delta(B_z^2/2\mu_0)$, in energy density of the axial field is $-B_z^2\Delta a/\mu_0 a$, where $\Delta a/a<0$. The corresponding change, $\Delta(B_\theta^2/2\mu_0)$, in the azimuthal field energy density is $B_\theta^2\Delta a/2\mu_0 a$. It follows that the net change in magnetic energy is positive if $B_z^2>\frac{1}{2}B_\theta^2$. This gives the required axial field strength necessary to stabilize the instability, as depicted in Fig. 21. Note that when the plasma tube is bent into a torus, one arrives at a simple model of the tokamak configuration.

The dual presence of both a poloidal field and a strong, vacuum toroidal field greatly improves the MHD stability of a toroidal pinch by eliminating both the sausage instability and the related bending instability shown in Fig. 22 and by introducing magnetic shear, which is useful in controlling pressure-driven instabilities. Indeed, the tokamak

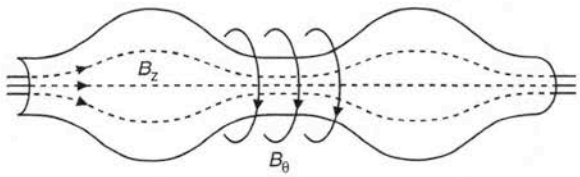

FIGURE 21 Stiffening of the Z pinch against sausage modes of instability by the addition of a field B_z along the plasma column (creating a screw pinch).

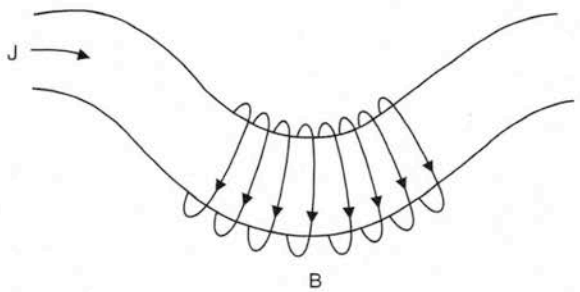

FIGURE 22 The bending mode of instability of the Z pinch. Note how the lines of force are crowded together on the inside of the bend and are moved apart on the outside of the bend; the concomitant difference in magnetic pressure acts to reenforce the displacement.

magnetic configuration is de facto defined by the pitch of its magnetic field lines, which is given by $q(r)=rB_\phi/R_0B_\theta$. With the (possible) exception of a finite region around the magnetic axis, the $q(r)$ of standard tokamaks exceeds 1 and increases with r so that the magnetic shear is positive. The maximum $q(r)$ in most standard tokamaks is between 2 and 4. The intrinsic dual periodicity of toroidal configurations means that perturbations also have their own effective pitch. This is a rational number, m/n, where m and n are positive integers, with m being the number of times the perturbation circles the torus in the poloidal direction while completing n turns in the toroidal direction. Thus, it is possible for the field line pitch $q(r)$ to equal (or resonate with) the perturbation pitch m/n at certain radii, $r_{m,n}$, where $q(r_{m,n})=m/n$. These special radii define magnetic surfaces that are called rational or resonant surfaces.

Resonant surfaces, and more generally field line pitch, are crucial to an important class of instabilities called kink-tearing instabilities. The onset of these instabilities is determined by $q(r)$ and by the radial gradient of the current profile. Since $q(r)$ is determined primarily by $B_\theta(r)$, kink-tearing instabilities are also conveniently described as current-driven instabilities. When the perturbation pitch m/n exceeds $q(a)$ for $r<a$, the instability does not involve magnetic reconnection and is called an external kink. It may then be described by ideal MHD. The effects of boundaries, particularly conducting walls, are vitally important to external kink dynamics and stability (see Section 4 and Fig. 9). When the perturbation is resonant [i.e., when $m/n=q(r)$ for $r<a$], reconnection is usually involved and the instability is called a tearing mode since magnetic field lines tear and reconnect. Tearing modes involve the formation of current filaments. In certain cases, the instability dynamics of a resonant kink (usually with $m=1$) can be described, at least in its initial phases, by ideal MHD. Such instabilities are called ideal internal kinks.

Ideal kink instabilities are current driven, but it is really the pitch of the magnetic field lines that signals the onset of the instability. Kink instabilities have long wavelength in the toroidal direction and cause the plasma column to snake helically around its equilibrium position in the manner shown in Fig. 23. Before the column is perturbed, the current flows parallel to the magnetic field. After perturbation, it follows the helical path shown and produces a magnetic field resembling that shown in Fig. 23. This is only part of the total field; to obtain the total field, one must imagine augmenting the B shown in the

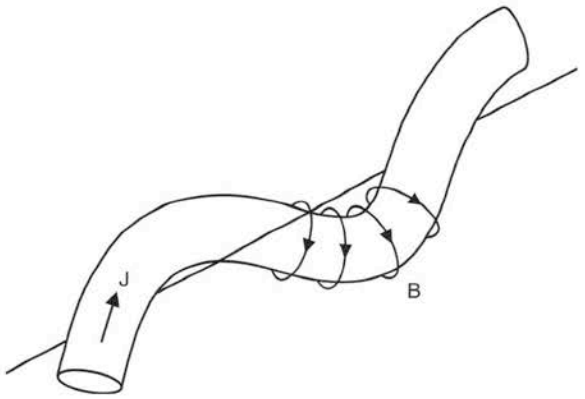

FIGURE 23 Kink instability of a toroidal equilibrium. In the initial state, the current flows along field lines. In the perturbed state (shown here), the current follows a helical path and creates a field, **B**, of the type shown. The remainder of the field (not shown) is along the helically distorted column. The net result is a field that has a component perpendicular to **J** that creates a Lorentz force enhancing the perturbation.

figure by the field along the column. The net result is a field, **B**, that has a component orthogonal to **J**. This creates a $\mathbf{J} \times \mathbf{B}$ force that reenforces the initial perturbation, thus promoting instability.

Kink instabilities are similar to the helical deformations of an elastic tube or band that occur when it is twisted beyond a critical value. An example of such kinks is sometimes seen on a wire connecting a telephone handset to its cradle. The twist of the band is clearly analogous to the initial pitch (or twist) of field lines, as given by $q(r)$. Kink instabilities reflect the tendency of the plasma to lower its energy by assuming a secondary, helical equilibrium that replaces the initial configuration with one of helical symmetry. The ultimate radial extent of the helical deformation is determined by several factors, including the amount of plasma current, the toroidal field strength, and the size of the gap between the plasma boundary and the conducting walls of the containment vessel. Since the plasma current channel expands during kink instabilities, these constitute a simple but very direct route to an undesirable disruption of the discharge, should the current column come into contact with a wall of the containment vessel.

In practice, external kink instabilities can be avoided by not operating the discharge with $q(a)$ close to a low-order rational number, such as, $\frac{3}{2}$, 2, or 3, and/or by having a conducting wall sufficiently close to the plasma column. Kink instabilities are also predicted to occur when $q(r) < 1$. For this reason, internal kinks are ubiquitous in tokamaks and are thought to be related to the sawtooth phenomenon. This refers to quasi-periodic relaxation oscillations of the central temperature of the tokamak that, in diagnostic recordings, produce a jagged trace reminiscent of the teeth on a saw.

Since internal kink perturbations usually do not pierce the plasma boundary or bring the current channel into contact with the vessel wall, they are usually not directly associated with disruptions. Internal kinks do, however, affect the performance of tokamaks by limiting the central plasma pressure that can be achieved.

The dynamics of energy release in resonant kinks or tearing modes are determined by nonideal effects (i.e., by effects that break the Alfvén frozen flux constraint). Typical of such nonideal effects is plasma resistivity η. However, it is important to keep in mind that the free energy source for tearing modes is the same as that for kinks, namely the current gradient. Nonideal effects, such as resistivity, are only the triggers of the instability and are significant only in a narrow diffusion layer, surrounding the resonant surface, in which reconnection occurs. Just as kinks tend to form helical secondary equilibria, so do tearing modes. However, since tearing modes are resonant, reconnection occurs, resulting in the formation of magnetic islands in the region near the resonant surface, as shown in Fig. 24. These islands may be thought of as consequences of current filamentation and concomitant reconnection. Magnetic islands are MHD analogues of Kelvin cat's eyes or nonlinear critical layers, which form as a consequence of certain hydrodynamic shear flow instabilities. When magnetic islands grow to a size at which they touch the wall, or when magnetic islands at neighboring resonant surfaces overlap (resulting in stochastic field lines in a region that pierces the surface of the plasma), MHD turbulence is generated, resulting in turbulent transport, rapid heat loss, and a sudden expansion of the current channel. When the current strikes the wall, a large impurity influx commences, and this raises the effective

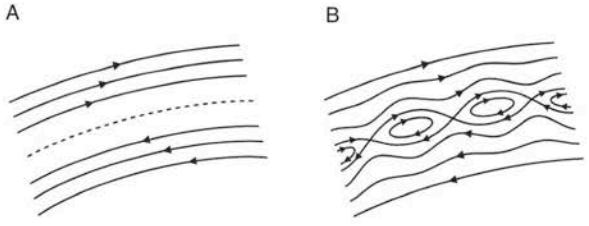

FIGURE 24 The formation of magnetic islands. (A) Initial state; the neutral line is shown dashed. (B) Field configuration after magnetic islands have formed around the neutral line.

plasma resistivity, which in turn quenches the current, creating a disruption. For this reason, tearing mode dynamics and stability are of great interest to MFE.

A final comment on tearing instabilities concerns their rate of growth. Ideal MHD instabilities grow exponentially, on Alfvénic (e.g., kink) or sonic (e.g., ballooning) timescales. Tearing modes initially grow at a rate proportional to $(\tau_A^{-2}\tau_\eta^{-3})^{1/5}$, where τ_A and τ_η are the Alfvén and (global) resistive diffusion times defined in Sections 3 and 4. Since $\tau_A \ll \tau_\eta$, tearing modes grow more slowly than ideal MHD modes. However, linear growth rates are of little relevance to the dynamics of the tearing mode since magnetic islands rapidly enter a nonlinear phase of algebraic growth. This occurs when the width of the magnetic island exceeds the width of the (narrow) reconnection layer of the linear theory. A major current research topic in tokamak MHD concerns the nonlinear growth and saturation of magnetic islands.

5.4 Interplay of MHD Instabilities and Tokamak Operation

Considerations of turbulent transport and MHD stability define the possible viable operating space of present-day tokamaks. The MFE program has sought to exploit understanding of MHD stability limits, etc. in order to expand and optimize the tokamak operating space. The tactics and tricks used include

1. *Shaping the cross section* to increase β limits: The goal here is to design a shape that increases the relative fraction of a magnetic field line that lies in the region of favorable curvature.
2. *Programming current and heating evolution* in order to avoid conditions that are prone to the onset of disruptions (i.e., in order to improve ideal stability limits).
3. *Controlling current profiles* by driving currents locally through the injection of radiofrequency waves.
4. *Using active feedback*, including current drive, to mitigate or retard the growth of undesirable perturbations.
5. *Driving plasma rotation* by neutral beam injection in order to stabilize certain MHD instabilities.

A recurrent theme in fusion research is the often rather diabolical ways in which various instabilities conspire to limit the operating space and tokamak performance. As mentioned previously, eliminating microinstabilities using transport barriers enhances confinement times but opens the door to pressure-driven instabilities (i.e., interchange ballooning modes). Operating at high current is good for energy confinement and helps limit pressure-driven ballooning modes, but it increases the possibility of disruption due to kink-tearing modes. Employing low currents improves stability but often degrades confinement and fails to achieve maximal machine performance. The list is long and continues to grow. These numerous and accumulating questions and concerns ensure that both the theoretical and experimental MHD of tokamaks and other MFE devices will remain vital and vibrant research areas well into the 21st century.

5.5 The Future of MHD in MFE

There is little doubt that in the near future the focus of the world MFE program will be the International Thermonuclear Experimental Reactor (ITER), a tokamak shown schematically in Fig. 25. The ITER program is an international project involving the collaboration of many countries. Its primary mission is to study plasma dynamics under conditions of a fusion burn, in which the main source of plasma heating is from collisional friction between the alpha particles produced by the thermonuclear reactions and the electrons.

A burning plasma is different from the standard electron–ion plasma discussed so far in (at least) two very important respects. First, a burning plasma contains a very substantial population of high-energy alpha particles. This situation is inconsistent with the foundations of MHD, which treats both ions and electrons together as a single fluid. The absolutely minimal viable theory of the dynamics of a burning plasma is a two-component description involving an MHD-like model of the bulk plasma and a kinetic equation for the energetic alphas; these have a velocity distribution that is far from Maxwellian and cannot therefore be adequately modeled by fluid equations. The two components of the model couple to each other electrodynamically.

The second important distinction between a burning plasma and a standard plasma is that high-energy alpha particles can resonate with plasma waves of higher frequency than can bulk particles, thus encouraging a new class of instabilities. Of particular importance among these are toroidal Alfvén eigenmodes (TAEs), which can be destabilized by resonance with alphas and so relax the alpha particle density and temperature gradients. TAEs are

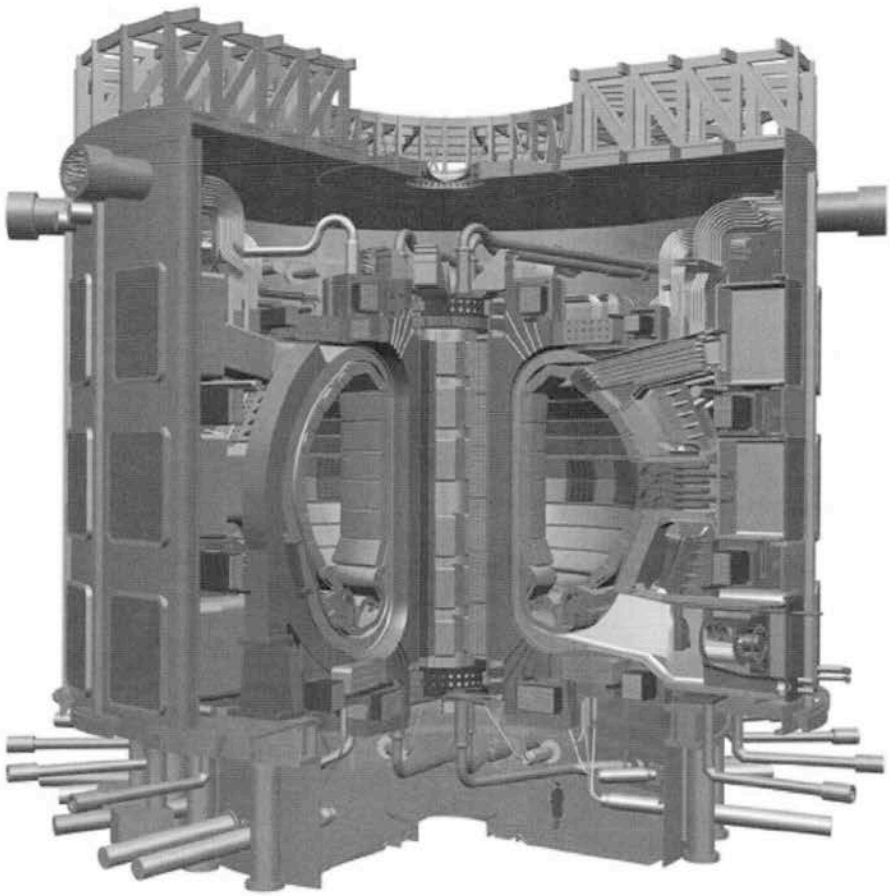

FIGURE 25 The tokamak ITER. To appreciate the scale of the device, see the figure of a person near the bottom.

critical to MFE since excessive instability-induced alpha losses can prevent, or prematurely quench, ignition. TAEs and other energetic particle-driven instabilities have been a topic of great interest in theoretical, computational, and experimental MFE research, with beams of externally injected high-energy particles used to simulate the effects of the alphas. Clearly, research in alpha particle-driven instabilities will be a major part of the ITER program.

Traditional MHD problems will be major foci of the ITER program as well. A key topic will certainly be feedback stabilization of instabilities, with the aim of avoiding or mitigating disruptions. Note that the disruption of a burning plasma could cause very significant damage to the ITER confinement vessel. Also, any successful fusion power plant must be effectively disruption free. Because the ITER plasma will be very hot, with concomitantly infrequent collisions between particles in the plasma, the traditional MHD model will need extension in order to include dynamical effects relevant to the ITER plasma. Such effects include possible nonideal, kinetic modifications to MHD as well as transport coefficients that describe dissipation due to micro-turbulence rather than collisions. Theoretical and computational research on such extended MHD models is being pursued vigorously throughout the world today. In addition, it is anticipated that subgrid scale models of turbulent transport will be an integral component of extended MHD models in the future.

SEE ALSO THE FOLLOWING ARTICLES

Electrical Energy and Power • *Electricity Use, History of* • *Electric Motors* • *Electromagnetism* • *Magnetic Levitation*

Further Reading

Bateman, G. (1978). "MHD Instabilities." MIT Press, Cambridge, MA.

Biskamp, D. (2003). "Magnetohydrodynamic Turbulence." Cambridge Univ. Press, Cambridge, UK.

Biskamp, D. (1997). "Nonlinear Magnetohydrodynamics." Cambridge Univ. Press, Cambridge, UK.

Chandrasekhar, S. (1961). "Hydrodynamic and Hydromagnetic Stability." Cambridge Univ. Press, Cambridge, UK.

Childress, S., and Gilbert, A. D. (1995). "Stretch, Twist, Fold: The Fast Dynamo." Springer, Heidelberg.

Davidson, P. A. (2001). "An Introduction to Magnetohydrodynamics." Cambridge Univ. Press, Cambridge, UK.

Drazin, P. G., and Reid, W. (1981). "Hydrodynamic Stability." Cambridge Univ. Press, Cambridge, UK.

Freidberg, J. P. (1987). "Ideal Magnetohydrodynamics." Plenum, New York.

Itoh, K., Itoh, S.-I., and Fukuyama, A. (1999). "Transport and Structure Formation in Plasmas." Institute of Physics Press, Bristol, UK.

Kadomtsev, B. B. (1992). "Tokamak Plasma: A Complex Physical System." Institute of Physics Press, Bristol, UK.

Krause, F., and Rädler, K.-H. (1980). "Mean-Field Magnetohydrodynamics and Dynamo Theory." Pergamon, Oxford, UK.

Mestel, L. (1999). "Stellar Magnetism." Oxford Univ. Press, Oxford, UK.

Parker, E. N. (1979). "Cosmic Magnetic Fields." Oxford Univ. Press, Oxford, UK.

Taylor, J. B. (1986). Relaxation and magnetic reconnection in plasmas. *Rev. Modern Phys.* **58**, 741–763.

Tillack, M.S., Morley, N.B. (1999). Magnetohydrodynamics. *In* "14th Standard Handbook for Electrical Engineer" (D. G. Fink and H. W. Beaty, Eds.), pp. 11-109–11-144. McGraw-Hill, New York.

Wesson, J. (1997). "Tokamaks." 2nd Ed. Oxford Univ. Press, Oxford, UK.

White, R. B. (1989). "Theory of Tokamak Plasmas." North-Holland, Amsterdam.